

[Reviewer's comments are inserted in regular font and responses are highlighted in blue. Relevant changes made in manuscript are also highlighted in blue.]

## **Responses to Reviewer #1**

### GENERAL COMMENTS

**Comment 1 (C1):** This manuscript investigates the mechanism controlling the development of hypoxia in the northern Gulf of Mexico with a modelling approach. The topics fit perfectly with the scope of Biogeosciences. The main question, i.e. to quantify the respective importance of the various oxygen sinks and sources in mitigating/enhancing hypoxia in the northern Gulf of Mexico, is well stated and modelling experiments well constructed to answer the question. The fact that stratification and sediment oxygen consumption are the main driver of hypoxia in this area has already been suggested but this manuscript specifically tests and confirms this hypothesis (by comparing hypoxic area obtained with and without considering water column biological processes affecting oxygen). The most problematic issue is the strong emphasis on benthic oxygen consumption in the discussion, and the large approximations in its representation in the model. Once the impact of the latter on the conclusions is discussed accordingly, this manuscript would constitute a valuable publication and contribution to the understanding of hypoxia in the northern Gulf of Mexico.

**Response (R):** We thank the reviewer for the encouraging comments. The emphasis on benthic oxygen consumption in the discussion is due to its critical importance as an oxygen sink in driving hypoxia on the LA shelf. We carefully addressed all specific comments, detailed below, which helped strengthen and improve the discussion.

**C2:** In general the manuscript is slightly redundant. There are many figures and all the information contained in the figure is not always exploited in the discussion. Either some figures could be removed, either these should be better integrated in the discussion.

**R:** We removed Figure 9, which was not fully exploited in the discussion, and further edited the manuscript to avoid redundancy.

### SPECIFIC COMMENTS

**C3:** [1] The main weakness of the modelling set-up lies in the empirical relationship used to estimate the sediment oxygen consumption (SOC). SOC is expressed as a direct function of bottom oxygen consumption, calibrated empirically on the basis of a set of in-situ benthic chambers measurements. While it is recognized (P14898 L15-21) that other SOC data sets indicate lower value than those obtained in the simulation (ie. Lehrter et al. 2012, Murrell and Lehrter, 2011) the manuscript states that "Observations from Rowe et al. (2002) and McCarthy et al. (2013) mostly fall within the range of the variability of simulated SOC". This has to be described more accurately since on Figure 7 only 4 points over a total of 12 (Rowe et al. (2002)) lie between the depicted range of 25th-75th model percentile, and 5/18 for McCarthy et al. (2013).

**R:** The sentence in question was removed and instead we now say (Page 13):

“Simulated SOC is at the upper range of the available observations.”

**C4:** [2] More generally, there is a paradox in that the validation procedure indicates simultaneously (1) an overestimation of bottom oxygen concentration and (2) an overestimation in sediment oxygen consumption (SOC). Moreover if we take into account the manuscript’s main conclusion which is that oxygen dynamics in the bottom layer is driven by sediment oxygen consumption. The direct (empirical) dependence of SOC on DO makes it difficult to interpret this behavior. The authors justify this (P14903,L22-P14904,L5) by suggesting that measured SOC could underestimate the true sediment oxygen demand, ie. that the accumulation of reduced metabolite resulting from benthic respiration could lead to further oxygen consumption not accounted for by SOC measurement. In order to be so, the oxidation of these metabolites should occur in the water column, which suppose those are released to the water column, which suppose quasi-anoxic bottom conditions, but Fig 7. indicates overestimated SOC over a large DO range. Could some physical aspects explain this apparent paradox? Can the accuracy of vertical diffusion at the bottom pycnocline and/or horizontal advection be checked independently, i.e. on the basis of physical aspects (probably this has been done already, and a referenced discussion will do). In general, because this is central to the main conclusion these aspects have to be discussed more completely.

**R:** We agree that the simultaneous overestimation of bottom oxygen concentration and SOC would be a paradox if SOC was the only process determining bottom oxygen dynamics and if our SOC parameterization was perfect. But, as indicated in the second half of the reviewer’s comment, of course other factors matter. A physical explanation would be that the bottom boundary layer in the model is too thick, which means that higher SOC rates are required to draw down bottom oxygen, than in reality. We added the following on page 19:

“Another explanation could be that the thickness of the simulated bottom boundary layer is overestimated. If this is the case, SOC would have to be larger than in reality in order to produce hypoxic bottom water. Future work on validating the expression and dynamics of the bottom boundary layer and its effect on hypoxia dynamics will address this question.”

**C5:** [3] I wonder why nitrification is listed in the oxygen sinks (P14895, L13) but is not considered in the budget (Section 3.3). Nitrification of ammonium originated from the sediments could be a significant oxygen sink in bottom waters not accounted for by SOC measurements. If nitrification happens to be a significant term in the budget and if in-situ estimates are available, a validation would greatly complete the present picture. For instance Lehrter et al. 2012 mention that "Realistic models of sediment O<sub>2</sub> dynamics for this shelf will need to include the accumulation of oxygen debt from reduced nitrogen, iron, manganese, and sulfur." In the present manuscript the list of "reduced metabolite" given P14903 excludes ammonium.

**R:** Unfortunately we didn’t make it clear enough in the text, but nitrification is explicitly included in the calculation of the dissolved oxygen balance (as a component of water

column respiration). We clarified this in the text (Page 14) as follow: “For simplicity, we are considering that oxygen consumption due to nitrification to be included in the respiration term, and not as a separate process for deriving the oxygen balance. Though we are referring to the sum of respiration and nitrification as WR, we recognize that nitrification is a chemoautotrophic process. While not strictly accurate, this is consistent with the use of WR in the observational literature where measurements of water column oxygen consumption include the contribution of nitrification.”

We also clarified it in the caption of Figure 9 for the oxygen balance (Page 47) by writing explicitly “respiration+nitrification.”

We also followed the suggestion of adding ammonium to the sentence on reduced metabolites (Page 18).

**C6:** [4] In general the effect of temperature on Oxygen saturation concentration should be acknowledged when discussing air-sea oxygen fluxes and community respiration/production (e.g. P 14900, L 1-3; P14901, L 15; P14905 L 4). For instance, which part of the oxygen flux to the atmosphere is due to the autotrophic condition of surface water, and which part is due to the fact that warming surface waters become naturally oversaturated in oxygen, as oxygen solubility decreases and exchanges rates at the surface are kinetically limited.

**R:** Agreed. In section 3.3 on page 14, we now say:

“In terms of air-sea exchange, oxygen is outgassing during summer and taken up during the rest of the year in all sub-regions, corresponding to the seasonal pattern in water column metabolism (more heterotrophic in winter and less heterotrophic or autotrophic in summer) and the seasonal cycle of surface water temperatures, which affect oxygen solubility contributing to outgassing in summer and uptake in winter.”

On Page 16 we now say:

“The positive net community production and decreasing oxygen solubility associated with the increasing water temperature in summer lead to oxygen outgassing to the atmosphere and net transport of oxygen downward to deeper waters.”

Also in section 4.2 on page 20 we now say:

“The decreased oxygen solubility of warmer waters typical of summer conditions also promotes outgassing, but the effect is relatively small compared to the autotrophy in surface waters (oxygen gas-exchange is fast and the summer change in water temperature is relatively small on the LA shelf). ”

We would also like to note that oxygen gas-exchange is fast and kinetic limitation negligible in this context. We have carried out sensitivity experiments where we doubled and halved the gas exchange coefficient and found only negligible changes in the results.

**C7:** [Table 3] The SOC bias is estimated by comparing model values to observations according to the DO ranges. This approach is strongly dependent on the assumption of a close relationship between SOC and DO, an assumption that is questioned by the large

dispersion of in-situ measurement depicted in Fig 7. Wouldn't it be better to compare model and in-situ SOC values according to the spatial distribution (e.g. using the four areas used in the present manuscript or the zones of similarity from Lehrter et al. 2012)? This could eventually lead to a discussion on the adequacy of using such a relationship over the important environmental gradient covered by the model domain. The validation procedure has to establish that the model approximation does not jeopardize the conclusions presented on the basis of the sensitivity experiment (i.e. with an without water column terms).

**R:** We have not found an along-shelf gradient in SOC. However, there is an across-shelf gradient with SOC increasing from inshore to offshore, which is driven by changes in bottom water oxygen concentrations such that offshore sites (in 50 m water depth) have higher SOC because of higher bottom water oxygen than inshore sites with lower bottom water oxygen. The SOC spread among the available different data sources is not due to a spatial pattern. Also, SOC measurements from all sources, except those from McCarthy et al. (2013), which were collected with a different method, show a dependence on oxygen concentration. Therefore we choose to compare model values with observations according to the DO ranges in Figure 7.

**C8:** [Fig. 5] Fig. 5 is not really exploited in the discussion. Why is this figure essential?

**R:** We feel that the vertical profiles of model bias in Figure 5 provide a good illustration of how model and data agree throughout the water column, and how the two simulations differ. Hence we chose to retain the figure to illustrate that point.

**C9:** [Fig 7.] SOC is a function of DO, modulated by temperature. As the same relationships is used in the two simulations (Model and MODEL + CCR), how comes that they depict different curves? Is that due to a different DO/Temperature distribution? Please clarify.

**R:** The physical model configuration is identical in the two simulations (i.e., the temperature distribution). At the same location and time, both model simulations have the same temperature, but the "Model+CCR" has lower DO concentrations. In Figure 7, at the same DO range, the SOC curve in "Model+CCR" corresponds to locations and times with lower temperatures than those in the "Model" and hence lower SOC values.

#### TECHNICAL COMMENTS

**C10:** [P14893, L11] Boyer et al, 2005 or 2006?

**R:** Corrected, it should be Boyer et al., 2006.

**C11:** [P14894 L 10] "Climatological boundary conditions were initialized using an average profile of temperature and salinity based on historical hydrographic data (Boyer et al., 2005) and assumed to be horizontally uniform": It is not clear with this sentence whether physical boundary conditions vary seasonally.

**R:** They don't vary seasonally. We have changed the sentence (page 7) as follows:

“An average profile of temperature and salinity, based on historical hydrographic data (Boyer et al., 2006) and assumed to be horizontally uniform, is used as physical boundary condition.”

**C12:** [P14899 L 18] Please provide the exact time frame of integration.

**R:** The sentence (Page 14) has been changed as follows: “In this section, we evaluate the DO balance for the summer period (June to August) for different regions of the LA shelf to identify the key processes controlling hypoxia.”

**C13:** [P14905 L 29] The reference Kemp et al. 1992 does not appear in the bibliography.

**R:** The reference is now added to the bibliography.

**C14:** [FIG 6.] Split the y-label: PP for the upper part; Water community respiration for the lower part.

**R:** Figure 6 was redone as suggested.

**C15:** [Fig. 9]: Should be introduced in section 3.1

**R:** In response to the reviewer's concern that there are too many figures, we removed Figure 9 ('Vertical distribution of hypoxia probability') and instead refer to Figure 6 in Fennel et al. (2013), which also shows that hypoxia most frequently occurs within a thin bottom water layer on the Louisiana shelf.

**C16:** [References] Refs Dagg et al., 2004; Green et al., 2006 ; Trefry et al., 1994 appears in the bibliography but not in the text

**R:** Removed.

## Responses to Reviewer #2

### GENERAL COMMENTS

**C1:** The manuscript analyses the output of a coupled physical-biogeochemical model with regard to oxygen distribution and variability at the Louisiana shelf. The strength of the study is the detailed validation of model results against different observations that nicely show the realism of the presented simulations. Main findings of the study are the important role of strong stratification shielding bottom layers from ventilation from above (associated with O<sub>2</sub> outgassing from the surface layer), a minor role of primary production below the pycnocline for the development of hypoxia on the shelf and that the hypoxia is determined by a combination of physical processes and sediment oxygen consumption. The last point, however, is in my mind somehow vague and it is not clear to me, how much it depends on the chosen parameterizations.

**R:** We appreciate the positive comments. Regarding how much our conclusion depends on the chosen parameterizations, we have carefully addressed the comments on sediment oxygen consumption and air-sea gas exchange parameterizations as detailed below and hope that the conclusions are better justified as a result.

**C2:** My main concern regards the parameterization of the sediment oxygen consumption (SOC) and the evaluation of the oxygen budget (Eq. 4-6). The used parameterization of SOC depends only on oxygen and temperature. This dependence clearly does not explain very well the observed variability of SOC (Fig. 7). As physical processes, particularly vertical diffusion, are the main oxygen supply to the bottom layer, the SOC parameterized by oxygen concentration depend on the strength of this oxygen supply. This could be an oversimplification of the problem. What could be the role of spatially varying available particulate organic matter on the shelf? Could this be accounted for or why we should not care about it? And is it correct to have a SOC parameterization that depends on oxygen concentration also for relatively high oxygen levels.

**R:** There are three points in this comment that we respond to separately:

1) Regarding “the SOC parameterization does not explain well the observed variability in SOC (Fig. 7)”

This is true and may partly be due to the different measurement techniques used (i.e. limitations in the available data) and partly because instantaneous SOC depends on many other factors (incl. for example sediment porosity and faunal activity), but there is no simple mechanistic formulation explaining these dependencies. The SOC parameterization we used, while simple, does include two parameters known to be key in modulating SOC: temperature, which is well-known to modulate the rate of microbial respiration in sediments, and dissolved oxygen concentration in the overlying water, which regulates the depth of O<sub>2</sub> diffusion into the sediments, and hence, the sediment O<sub>2</sub> flux into the sediments (Cai and Sayles 1996). The SOC parameterization has been used in previous modeling studies in this region and shown to accurately simulate hypoxia relative to observations. The discrepancies between the parameterization and the observed rates are a subject of our Discussion and will, without a doubt, be the subject of future research.

2) Regarding “What could be the role of spatially varying particulate organic matter [flux]? Could this be accounted for or why should we not care about it?”

We have a model configuration where SOC was determined by the amount of organic matter sinking to the sediment (this was used in several of our previous publications) and we have actually performed all analyses presented in this manuscript for these simulations as well (and they were part of the very first draft of this manuscript). It turned out, however, that our conclusions about the summer oxygen balance are essentially identical when using the spatially and temporally varying organic matter flux to the sediment rather than the SOC parameterization. We decided it would be too tedious and redundant to report results for both cases and since the model’s skill in simulating hypoxia is better when using the latter (see e.g. Fennel et al. 2013) we chose to show those. We state this now in section 4.1 on Page 19.

3) Regarding “is it correct to have a SOC parameterization that does depend on SOC for relatively high oxygen levels?”

SOC is dependent on oxygen concentration only for low oxygen levels. We added the following text in the description of our SOC parameterization (Page 10):

“SOC linearly increases with increasing bottom water *DO* for concentrations lower than 50 mmol O<sub>2</sub> m<sup>-3</sup> and saturates when concentrations are higher than 100 mmol O<sub>2</sub> m<sup>-3</sup>.” This characteristic is shown in Figure 7 where the simulated SOC increases with increasing bottom DO for oxygen concentrations below ~50 mmol O<sub>2</sub> m<sup>-3</sup>. The reason the SOC declines above ~80 mmol O<sub>2</sub> m<sup>-3</sup> in Fig. 7 is its temperature dependence (high oxygen concentrations occur in winter when water is colder).

**C3:** The oxygen budget for the three layers described by equation 4 to 6 is not easy to understand and to follow. I would suggest writing down more complete equations. My concerns are the following. If you integrate the time derivative of oxygen over volume and time (first term of equation 4-6, respectively), you obtain the amount of mol O<sub>2</sub> within the volume of integration. My understanding from your description is that this volume is not constant for the upper and middle layer. Thus volume changes have to be incorporated into the equations. This also includes the question, what happens if during part of the time only two layers exist and the budget is not evaluated (P14900, L10)? This would change the mol O<sub>2</sub> in the regional budgets.

**R:** We replaced all occurrences of ‘oxygen budget’ with ‘oxygen balance’, because we feel the latter is a more accurate description of our calculations for the reasons mentioned by the reviewer. We have also removed equations 4-6 that caused confusion; instead, we added the equation of DO conservation in section 2 (‘Model description’) and clarified how we calculated the summer oxygen balance in section 3.3:

(Page 9) “The equation for the *DO* conservation is given by

$$\frac{\partial DO}{\partial t} = - \left( u \frac{\partial DO}{\partial x} + v \frac{\partial DO}{\partial y} + w \frac{\partial DO}{\partial z} \right) + \frac{\partial}{\partial z} \left( K_v \frac{\partial DO}{\partial z} \right) + PP + WR + F_{bf} \quad (1)$$

where *x* and *y* represent the two horizontal directions and *z* the vertical direction, *u*, *v*, and *w* (m s<sup>-1</sup>) represent velocities in *x*-, *y*-, and *z*-directions, respectively, and *K<sub>v</sub>* is the vertical

diffusivity ( $\text{m s}^{-2}$ ). On the right-hand side of the Eq. (1), the first term represents horizontal and vertical advection of DO, and the second term is the vertical diffusion of DO (horizontal diffusivity  $K_H$  is set 0 in the model and hence we neglected horizontal diffusion terms in equation). Here the advection and diffusion terms are computed using the advanced numerical schemes build into the ROMS hydrodynamic model. The term PP is the primary production and WR represents the sum of water column respiration and nitrification. Although not strictly accurate, the use of the terminology WR is consistent with the use of WR in the observational literature where measurements of water column oxygen consumption include the contribution of nitrification. The term  $F_{bf}$  represents the boundary oxygen fluxes, namely the air-sea flux of oxygen at the top layer and the sediment oxygen consumption at the bottom layer, the parameterizations of which are detailed below.”

(Page 15) “We defined the pycnocline as the depth of maximum Brunt-Vaisala Frequency (Pond and Pickard, 1983) and restricted our analysis to horizontal grid cells where all three layers existed (i.e. a main pycnocline was present and was more than 5 m above the bottom). We then integrated the terms in Eq. (1) vertically over each layer at each desired grid cell on each desired day. The advection and diffusion terms were evaluated as divergences, namely fluxes of DO into or out of the given volume through advection or diffusion. Finally we averaged the integrated results over all grid cells within a selected sub-region and over June to August in order to obtain the summer oxygen balance for the sub-regions.”

**C4:** Moreover, it is not clear how the advection and diffusion term in the oxygen budget are evaluated. The calculation of the supply due to horizontal advection (which is part of the advection terms, P14901, L6-7) is not correct, as it is written. The integration must be over vertical planes, e.g.  $u$  times O2 integrated over  $y$  and  $z$  and  $v$  times O2 integrated over  $x$  and  $z$ . Moreover, it is not clear to me if these integrations are done for each grid cell or for the whole region. Thus it would be really helpful to see more detailed equations that also would better explain the other terms. How is the vertical diffusion parameterized? Do you use a horizontal diffusivity in the tracer equation? Why it is not included in the budget? Are you able to close the budget with your calculations? What is the error in budget calculations?

**R:** In the ROMS model, advection and diffusion diagnostics were calculated as divergences, namely fluxes of DO into or out of a given volume (i.e. grid cell), and not as fluxes through vertical planes. (This is why vertical and horizontal advection in Figure 9 cannot be separated.) The ROMS diagnostics were calculated in this way because it is practically impossible to close tracer budgets if fluxes are approximated as fluxes across horizontal and vertical planes. However, when using divergences, tracer budgets close perfectly.

We have added the equation of DO conservation in section 2 (‘Model description’):

$$\frac{\partial DO}{\partial t} = - \left( u \frac{\partial DO}{\partial x} + v \frac{\partial DO}{\partial y} + w \frac{\partial DO}{\partial z} \right) + \frac{\partial}{\partial z} \left( K_v \frac{\partial DO}{\partial z} \right) + PP + WR + F_{bf} \quad (1)$$

To calculate oxygen balance, we integrated the terms in Eq. (1) vertically over each layer at each desired grid cell on each desired day. We then averaged the oxygen balance over the grid cells within a selected sub-region and over June to August to obtain the summer oxygen balance. Please see the response to comment 4 for more details on the calculations.

The vertical mixing is parameterized using the Mellor and Yamada (1982) turbulent closure scheme.

Horizontal diffusivity is set as 0 in the model and hence horizontal diffusion term is not included in the oxygen balance.

We have also added more details in Section 2 Model description (Page 7): “The model uses a fourth-order horizontal advection scheme for tracers and a third-order upwind scheme for the advection term in the momentum equation. Vertical gradients are calculated with conservative parabolic splines, and vertical mixing is parameterized using the Mellor and Yamada (1982) turbulent closure scheme.”

**C5:** In general, it would be helpful to see some discussion on the sensitivity of the model results to different parameterizations, e.g. the air-sea gas parameterizations. What is the uncertainty of the model results due to the use of these specific parameterizations? Other specific points are listed below. In summary, I think that this paper could be good contribution to a better understanding of low oxygen regions and particularly to the hypoxia of Louisiana after clarification of the addressed general remarks above and specific points below.

**R:** We have added a discussion of the effect of the air-sea gas exchange parameterization in the revision (Page 20):

“We have carried out sensitivity experiments where we doubled and halved the air-sea gas exchange coefficient (results not presented in the manuscript) and found that the model results are insensitive to the air-sea gas exchange rates, likely because the air-sea oxygen flux is fast.”

#### SPECIFIC POINTS

**C6:** P14890, L14: “autotrophic/heterotrophic water” sounds not ok, please reformulate

**R:** We modified this sentence (Page 2) in the abstract by removing the second part that contained autotrophic and heterotrophic. It now reads: “During this time, efflux of oxygen to the atmosphere, driven by photosynthesis and surface warming, becomes a significant oxygen sink.”

**C7:** P14891, L29: Do you have explicit horizontal (isopycnal) diffusion in the tracer equation? How is it parameterized? It would be helpful to see the equations that are evaluated for the budget. See also my points above.

**R:** No, the horizontal diffusion coefficient is zero in the model. Also see the response to

comment 4.

**C8:** P14894, L12: You use horizontal uniform T/S boundary conditions, which does not allow baroclinic inflow. What are your conditions for flow into and out of the model domain? How do you account for larger scale advection?

**R:** We added more details on how the physical horizontal boundaries are treated:

(Page 7) “An average profile of temperature and salinity, based on historical hydrographic data (Boyer et al., 2006) and assumed to be horizontally uniform, is used as physical boundary condition. At the three open boundaries, gradient conditions are used for the free surface, radiation conditions for the three-dimensional velocities, and a Flather (1976) condition with no mean barotropic background flow for the two-dimensional velocities.”

(Page 7) “The model uses a fourth-order horizontal advection scheme for tracers and a third-order upwind scheme for the advection term in the momentum equation.”

**C9:** P14895, L25: Wanninkhof (1992) proposed a parameterization with relatively large air-sea gas exchange. Particularly in high productive upwelling regions, the air-sea gas exchange might be limited by surface films (Tsai and Liu, 2003). Probably the effect on hypoxia would be very minor, when using different parameterizations. Please comment on that.

**R:** We are confident that the effect is negligible. Please see the response to comment 5.

**C10:** P14896, L7: Dependence of SOC on oxygen concentration is typically assumed for much lower oxygen levels only (e.g. Canfield 1993, 1994). Why is there no dependence on organic matter load?

**R:** Please see the response to comment 2.

**C11:** P14901, Eq. 6: Terms for horizontal and vertical advectations has to be separated and integrated over different planes.

**R:** Advection terms are calculated from divergences, hence can not be separated into horizontal and vertical. Please see the response to comment 4.

**C12:** P14972, Figure 10: Please explain the term “Net”.

**R:** We have added an explanation in the caption of this Figure (Page 47, now Figure 9): “The net rate of oxygen change in each layer (i.e. the sum of all oxygen source and sink terms) is given and denoted as Net.”

Cai W.J., and Sayles F.: Oxygen penetration depths and fluxes in marine sediments,

Marine Chemistry, 52, 123-131, 1996.

Canfield, D. E.: Organic matter oxidation in marine sediments, in: Interactions of C, N, P and S Biogeochemical Cycles and Global Change, edited by: Wollast, R., Mackenzie, F. T., and Chou, L., NATO ASI Ser. I, 4, 333–364, Springer, Berlin, 1993.

Canfield, D.E.: Factors influencing organic carbon preservation in marine sediments, Chem. Geol., 114, 315–329, 1994.

Fennel, K., Hu, J., Laurent, A., Marta-Almeida, M., and Hetland, R.D.: Sensitivity of hypoxia predictions for the Northern Gulf of Mexico to sediment oxygen consumption and model nesting, J. Geophys. Res., 118, 990-1002, 2013.

Tsai, W. T. and Liu, K. K.: An assessment of the effect of sea surface surfactant on global atmosphere-ocean CO<sub>2</sub> flux, J. Geophys. Res.-Oceans, 108, 3127, doi:10.1029/2000jc000740, 2003.



6 **Abstract**

7 The Louisiana shelf in the northern Gulf of Mexico receives large amounts of freshwater  
8 and nutrients from the Mississippi/Atchafalaya River system. These river inputs  
9 contribute to widespread bottom-water hypoxia every summer. In this study, we use a  
10 physical-biogeochemical model that explicitly simulates oxygen sources and sinks on the  
11 Louisiana shelf to identify the key mechanisms controlling hypoxia development. First,  
12 we validate the model simulation against observed dissolved oxygen concentrations,  
13 primary production, water column respiration, and sediment oxygen consumption. In the  
14 model simulation, heterotrophy is prevalent in shelf waters throughout the year except  
15 near the mouths of the Mississippi and Atchafalaya Rivers where primary production  
16 exceeds respiratory oxygen consumption during June and July. **During this time, efflux**  
17 **of oxygen to the atmosphere, driven by photosynthesis and surface warming, becomes a**  
18 **significant oxygen sink.** A substantial fraction of primary production occurs below the  
19 pycnocline in summer. We investigate whether this primary production below the  
20 pycnocline is mitigating the development of hypoxic conditions with the help of a  
21 sensitivity experiment where we disable biological processes in the water column (i.e.  
22 primary production and water column respiration). In this experiment below-pycnocline  
23 primary production reduces the spatial extent of hypoxic bottom waters only slightly. Our  
24 results suggest that the combination of physical processes and sediment oxygen  
25 consumption largely determine the spatial extent and dynamics of hypoxia on the  
26 Louisiana shelf.

## 27 **1. Introduction**

28 The Louisiana shelf (LA shelf) in the northern Gulf of Mexico receives large inputs of  
29 freshwater, nutrients and organic matter from the Mississippi/Atchafalaya River system  
30 and experiences widespread hypoxia (oxygen concentrations  $< 2 \text{ mg l}^{-1}$  or  $62.5 \text{ mmol m}^{-3}$ )  
31 <sup>3</sup>) in bottom waters every summer (Rabalais et al. 2007; Bianchi et al. 2010). The classic  
32 paradigm for explaining the recurring hypoxic conditions on the LA shelf is that high  
33 nutrient inputs from the river stimulate high rates of primary production in coastal waters;  
34 as this organic matter sinks below the pycnocline and is respired, dissolved oxygen (DO)  
35 becomes depleted due to a combination of high microbial respiration and low re-  
36 oxygenation of the bottom waters because of strong stratification (Rabalais et al. 2002).

37 While the statistical linkage between spring nutrient loads and the spatial extent of the  
38 summer hypoxic area is well documented (Turner et al., 2005; Greene et al., 2009;  
39 Forrest et al., 2011), the distribution of hypoxia on the LA shelf is known to be the  
40 integrated result of various physical and biogeochemical processes that interact non-  
41 linearly (Bianchi et al. 2010; Fennel et al. 2011). Rowe and Chapman (2002) suggested  
42 that as the distance from the river mouth increases, the primary driver of hypoxia changes  
43 from deposition of riverine organic matter to biological production and respiration and  
44 finally to physical stratification. Model simulations (Bierman et al., 1994; Breed et al.,  
45 2004; Eldridge and Roelke 2010) also show that the dominant processes contributing to  
46 hypoxia change in westward direction, namely allochthonous organic matter accounts for  
47 most of DO consumption near the Mississippi river mouth and autochthonous organic  
48 matter dominates DO consumption farther west. Hetland and DiMarco (2008) suggested  
49 that the differences in vertical stratification within the Mississippi and Atchafalaya River

50 plumes lead to differences in the dominant type of respiration responsible for hypoxia  
51 with water column respiration driving hypoxia near the Mississippi River plume and  
52 benthic respiration controlling hypoxia near Atchafalaya Bay and further west. Recent  
53 work suggests that the main axis of variability in hydrography and metabolism is inshore  
54 to offshore on the shelf (Lehrter et al. 2012; Murrell et al., 2013a; Lehrter et al., 2013;  
55 Fry et al., 2014).

56 Understanding the occurrence of hypoxia on the LA shelf requires quantitative  
57 knowledge of the mechanisms controlling DO dynamics. Generally, the distribution of  
58 DO is determined by physical processes (air-sea flux, horizontal advection, vertical  
59 mixing across the pycnocline) and biogeochemical processes (photosynthetic production,  
60 respiration in the water column and sediments, and oxidation of reduced substances)  
61 (Testa and Kemp, 2011). The magnitudes and spatial and temporal dynamics of these  
62 processes on the LA shelf are as of now poorly constrained.

63 Circulation over the LA shelf displays two distinct modes (Cochrane and Kelly, 1986;  
64 Cho et al., 1998): an upcoast circulation mode during the dominantly upwelling-favorable  
65 (westerly) winds in summer (June to August) versus westward flow during the  
66 dominantly downwelling-favorable (easterly) winds for the rest of the year. Previous  
67 statistical studies (Forrest et al., 2011; Feng et al., 2012) have shown that the observed  
68 hypoxic extent is correlated to the duration of upwelling-favorable wind. Feng et al.  
69 (2014) further showed that the wind influences the distribution of low salinity, high  
70 chlorophyll water on the shelf and thereby the bottom water DO concentrations and  
71 hypoxic area.

72 A substantial fraction of phytoplankton production is observed below the pycnocline  
73 (Lehrter et al., 2009) and even at the sediment-water interface when light is available  
74 (Lehrter et al., 2014), but the effect of sub-pycnocline production on bottom water  
75 hypoxia is not well known. Eldridge and Morse (2008) highlighted the importance of  
76 benthic respiration as a DO sink at the beginning and end of hypoxic events, and  
77 suggested water column respiration in bottom water near the pycnocline as primary O<sub>2</sub>  
78 sink once hypoxia has developed. Quinones-Rivera et al. (2007, 2010) estimated benthic  
79 respiration to account for ~73% of the total DO loss within 1 m of the bottom sediments  
80 during summer based on  $\delta^{18}O$  measurements and an isotope fractionation model,  
81 whereas Murrell and Lehrter (2011) found that benthic respiration only contributes on  
82 average  $20\pm 4\%$  of total respiration below the pycnocline. The relative contributions of  
83 benthic and water column respiration are strongly affected by the assumed depth of the  
84 bottom layer.

85 In order to better understand the relative importance of these processes, considerable  
86 efforts have been invested in modeling the DO dynamics and hypoxia within the system.  
87 These models range from relatively simple regression models (Turner et al., 2005, 2006;  
88 Greene et al., 2009; Forrest et al., 2011; Feng et al. 2012) to more complex process  
89 simulations that emphasize either biogeochemical processes in simplified physical  
90 frameworks (Justić et al. 1996, 2002; Eldridge and Morse, 2008; Green et al. 2008) or  
91 physical circulation using detailed hydrographic models with simple parameterizations of  
92 biogeochemical process (Hetland and DiMarco 2008; Lehrter et al., 2013). More recently  
93 a number of fully coupled physical-biogeochemical models have become available  
94 (Fennel et al. 2013; Laurent and Fennel 2014; Feng et al. 2014; Justić and Wang 2014).

95 Coupled models of DO dynamics and circulation have been used successfully in other  
96 coastal systems with seasonal hypoxia including Chesapeake Bay (i.e., Cerco and Cole,  
97 1993; Cerco, 1995). More recently, Li et al. (2015) coupled an empirical DO model  
98 derived from observations with a high-resolution hydrodynamic model to derive a DO  
99 budget for Chesapeake Bay. An even simpler empirical DO parameterization was used by  
100 Scully (2013) to illustrate the important role of physical forcing in the formation of  
101 seasonal hypoxia. Both, Li et al. (submitted) and Scully (2013) obtained a realistic  
102 simulation of the seasonal cycle of DO and spatial distributions of hypoxic water.

103 Here we use a coupled physical-biogeochemical model for the LA shelf described in  
104 Fennel et al. (2011, 2013) that was recently extended to include phosphate by Laurent et  
105 al. (2012) and Laurent and Fennel (2014). The biogeochemical model explicitly simulates  
106 DO and is coupled to the realistic 3-dimensional circulation model of Hetland and  
107 DiMarco (Hetland and DiMarco 2008, Hetland et al. 2012). Here we build upon the  
108 earlier work to identify the key processes controlling DO dynamics.

109 The manuscript is organized as follows. First we describe the coupled physical-  
110 biogeochemical model and its DO source and sink terms. Then we validate model-  
111 simulated DO and oxygen production and consumption rates against available  
112 observations. We explore spatial and temporal patterns of water column metabolism  
113 across the shelf and its interaction with air-sea fluxes. We also analyze the summer DO  
114 balance for different regions which allows us to identify the key controlling processes and  
115 how they vary in space. Finally, we examine the role that sub-pycnocline primary  
116 production plays in hypoxia generation.

117

## 118 2. Model description

119 Our physical model is the Regional Ocean Modelling System (Haidvogel et al. 2008,  
120 ROMS, <http://myroms.org>) configured for the Mississippi/Atchafalaya outflow region as  
121 described in Hetland and DiMarco (2008, 2012). The model grid covers the Louisiana  
122 continental shelf with a horizontal resolution ranging from ~20 km in the southwestern  
123 corner to 1 km near the Mississippi Delta, and has 20 terrain-following vertical layers  
124 with increased resolution near the surface and bottom (Fig. 1). The model uses a fourth-  
125 order horizontal advection scheme for tracers and a third-order upwind scheme for the  
126 advection term in the momentum equation. Vertical gradients are calculated with  
127 conservative parabolic splines, and vertical mixing is parameterized using the Mellor and  
128 Yamada (1982) turbulent closure scheme. An average profile of temperature and salinity,  
129 based on historical hydrographic data (Boyer et al., 2006) and assumed to be horizontally  
130 uniform, is used as physical boundary condition. At the three open boundaries, gradient  
131 conditions are used for the free surface, radiation conditions for the three-dimensional  
132 velocities, and a Flather (1976) condition with no mean barotropic background flow for  
133 the two-dimensional velocities. The model is forced with 3-hourly winds from the NCEP  
134 North American Regional Reanalysis (NARR) and climatological surface heat and  
135 freshwater fluxes from da Silva et al. (1994a, b). Freshwater inputs from the Mississippi  
136 and Atchafalaya rivers are based on daily measurements of transport by the US Army  
137 Corps of Engineers at Tarbert Landing and Simmesport, respectively.

138 The biological component of the model uses the nitrogen cycle model of Fennel et al.  
139 (2011, 2013) but was extended to include phosphate (Laurent et al., 2012) and river  
140 dissolved organic matter as additional state variables. The model is a relatively simple

141 representation of the pelagic nitrogen (N) cycle, including two species of dissolved  
142 inorganic N, nitrate ( $\text{NO}_3$ ) and ammonium ( $\text{NH}_4$ ), phosphorus ( $\text{PO}_4$ ), one phytoplankton  
143 group (Phy), chlorophyll (Chl) as a separate state variable to allow for photoacclimation,  
144 one zooplankton group (Zoo), two pools of detritus representing large, fast-sinking  
145 particles (LDet), and suspended, small particles (SDet), and river-born dissolved organic  
146 matter (RDOM). Combined with the freshwater discharge described above, the model  
147 receives river nutrients ( $\text{NO}_3$  and  $\text{NH}_4$ ) and organic matter based on the US Geological  
148 Survey (USGS) estimates (<http://toxics.usgs.gov/>). More specifically, river dissolved  
149 organic nitrogen (DON) was determined as the difference between filtered Total Kjeldahl  
150 Nitrogen (TKN) and  $\text{NH}_4$ ; and particulate organic nitrogen (PON) was defined as the  
151 difference between unfiltered and filtered TKN (Fig. 2). Different from our previously  
152 published simulations where river organic nitrogen enters the pool of SDet in the model  
153 without distinguishing between dissolved and particulate fractions, here river DON and  
154 PON enter the pools of RDOM and SDet, respectively. The only biological term in the  
155 equation for RDOM is remineralization to  $\text{NH}_4$  in the water column. We chose a  
156 remineralization rate of  $0.03 \text{ d}^{-1}$  for RDOM, an order of magnitude lower than that of  
157 small detritus ( $0.3 \text{ d}^{-1}$ ) to reflect the observation that riverine dissolved organic matter is  
158 less labile than phytoplankton-derived organic matter (Shen et al., 2012). A schematic of  
159 the extended N cycle model is shown in Figure 3. Also shown are the biological sources  
160 and sinks of DO, including photosynthetic production, nitrification, respiration in water  
161 column and sediment, and the air-sea flux of oxygen across the air-sea interface. At the  
162 open boundaries  $\text{NO}_3$ ,  $\text{PO}_4$  and oxygen were prescribed using the NODC World Ocean  
163 Atlas. All other biological state variables at the boundary were set to small positive

164 values. Model parameterization and previous validations were described in Fennel et al.  
165 (2006, 2011, 2013), Laurent et al. (2012), Laurent and Fennel (2014). For completeness'  
166 sake, all parameter values are given in Table S1 of the Online Supplement.

167 The equation for the *DO* conservation is given by

$$168 \quad \frac{\partial DO}{\partial t} = - \left( u \frac{\partial DO}{\partial x} + v \frac{\partial DO}{\partial y} + w \frac{\partial DO}{\partial z} \right) + \frac{\partial}{\partial z} \left( K_v \frac{\partial DO}{\partial z} \right) + PP + WR + F_{bf} \quad (1)$$

169 where  $x$  and  $y$  represent the two horizontal directions and  $z$  the vertical direction,  $u$ ,  $v$ , and  
170  $w$  ( $\text{m s}^{-1}$ ) represent velocities in  $x$ -,  $y$ -, and  $z$ -directions, respectively, and  $K_v$  is the vertical  
171 diffusivity ( $\text{m s}^{-2}$ ). On the right-hand side of the Eq. (1), the first term represents  
172 horizontal and vertical advection of DO, and the second term is the vertical diffusion of  
173 DO (horizontal diffusivity  $K_H$  is set 0 in the model and hence we neglected horizontal  
174 diffusion terms in equation). Here the advection and diffusion terms are computed using  
175 the advanced numerical schemes build into the ROMS hydrodynamic model. The term  
176 PP is the primary production and WR represents the sum of water column respiration and  
177 nitrification. Although not strictly accurate, the use of the terminology WR is consistent  
178 with the use of WR in the observational literature where measurements of water column  
179 oxygen consumption include the contribution of nitrification. The term  $F_{bf}$  represents the  
180 boundary oxygen fluxes, namely the air-sea flux of oxygen at the top layer and the  
181 sediment oxygen consumption at the bottom layer, the parameterizations of which are  
182 detailed below.

183 Following Fennel et al. (2013), an air-sea flux of oxygen ( $F_{air-sea}$ , in units of  $\text{mmol}$   
184  $\text{O}_2 \text{ m}^{-2} \text{ d}^{-1}$ ) is prescribed in the top layer of the model as:

$$185 \quad F_{air-sea} = \frac{vk_{O_2}}{\Delta z} (DO_{sat} - DO), \quad (2)$$

186 where  $DO$  and  $DO_{sat}$  are the oxygen concentration and concentration at saturation,  
187 respectively,  $\Delta z$  is the thickness of the respective grid box, and  $vk_{O_2}$  is the gas exchange  
188 coefficient for oxygen based on Wanninkhof (1992), such that:

$$189 \quad vk_{O_2} = 0.31 u_{10}^2 \sqrt{\frac{660}{Sc_{Ox}}}, \quad (3)$$

190 where  $u_{10}$  is the wind speed at 10 m above the sea surface, and  $Sc_{Ox}$  is the Schmidt  
191 number, calculated as in Wanninkhof (1992).

192 The parameterization for Sediment Oxygen Consumption (SOC) used in this study was  
193 developed by Hetland and DiMarco (2008) and based on observed sediment oxygen  
194 fluxes from Rowe et al. (2002). In this parameterization, SOC ( $mmol O_2 m^{-2} d^{-1}$ ) linearly  
195 increases with increasing bottom water oxygen ( $DO$ ,  $mmol O_2 m^{-3}$ ) for concentrations  
196 lower than  $50 mmol O_2 m^{-3}$  and saturates when concentrations are higher than  $100 mmol$   
197  $O_2 m^{-3}$ . Also, SOC is dependent on temperature ( $T$ ,  $^{\circ}C$ ) such that it doubles for every  $10^{\circ}C$   
198 temperature increase (i.e.,  $Q_{10} = 2$ ). The equation is given as follows:

$$199 \quad SOC = 6 [mmol O_2 m^{-2} d^{-1}] * 2^{T/10^{\circ}C} * (1 - \exp\left(-\frac{DO}{30[mmol O_2 m^{-3}]}\right)). \quad (4)$$

200 In Fennel et al. (2013) this parameterization was extended to include an  $NH_4$  flux into  
201 the bottom water proportional to oxygen uptake by the sediments. Therefore, organic  
202 matter sinking out of the water column essentially leaves the system while empirically  
203 determined fluxes of oxygen into the sediments and ammonium out of the sediments are  
204 prescribed.

205 Motivated by the model-data comparisons, described below, we conducted a sensitivity  
206 experiment where a spatially and temporally constant oxygen consumption rate (1.5

207 mmol O<sub>2</sub> m<sup>-3</sup> d<sup>-1</sup>) was added to the water column oxygen pool (simulation denoted as  
208 ‘Model+CCR’). In order to distinguish between the role of biological processes in the  
209 water column (primary production and water column respiration, denoted as PP and WR,  
210 respectively) and the combination of physical transport and sediment respiration, we  
211 conducted two further sensitivity experiments where all biological processes in the water  
212 column were turned off (denoted as ‘Model w/o PP and WR’ and ‘Model+CCR w/o PP  
213 and WR’ in comparison to the full model simulation and Model+CCR, respectively).

214 All simulations were run from 1 January 2004 to 31 December 2007. For model  
215 analysis we defined four geographical zones across the Louisiana continental shelf: three  
216 sub-regions associated with the Mississippi River plume (Mississippi Delta, Mississippi  
217 Intermediate, Mid-shelf), and another sub-region associated with the Atchafalaya River  
218 plume (Atchafalaya Plume) (Fig. 1). These four sub-regions cover most stations that  
219 comprise the observational data sets used for model validation: (1) DO concentrations  
220 from Rabalais et al. (2007), Nunally et al. (2013), Murrell et al. (2013b), and the  
221 Mechanisms Controlling Hypoxia (MCH) program; (2) in situ measurements of water  
222 column respiration rates from 10 cruises during spring, summer and fall from 2003 to  
223 2007 (Murrell et al., 2013a); (3) the concurrent measurements of phytoplankton  
224 production from Lehrter et al. (2009); (4) benthic flux measurements from Rowe et al.  
225 (2002), Murrell and Lehrter (2011), Lehrter et al. (2012), and McCarthy et al. (2013).  
226 Locations for the observed primary production and water column respiration rates are  
227 shown as black dots in Figure 1.

228

### 229 **3. Results**

230 **3.1 Simulated oxygen dynamics and model validation**

231 Time series of simulated and observed bottom DO both show a seasonal cycle reaching  
232 a maximum between December and February and minimum between July and August  
233 (Fig. 4). In summer the median of simulated bottom DO is consistently larger than  
234 observations in the Mississippi Intermediate region, but otherwise observations and  
235 simulation agree well. Simulated bottom DO falls within the observed range of variability  
236 for all 4 regions.

237 We report model bias and root mean square error (RMSE) as statistical measures of  
238 agreement between simulated and observed bottom DO in Table 1. Bias was calculated as  
239 model minus observations; thus a positive bias indicates that the model overestimates the  
240 observations. Table 1 indicates that the model overestimates the observed bottom DO in  
241 all regions with an average bias of 33.7 mmol O<sub>2</sub> m<sup>-3</sup>. Based on this comparison, the  
242 model performs best in the Mid-shelf region (bias of 15.6 mmol O<sub>2</sub> m<sup>-3</sup>) and worst in the  
243 Mississippi Delta region (bias of 43.3 mmol O<sub>2</sub> m<sup>-3</sup>).

244 Profiles of bias between simulated and observed DO profiles are shown in Figure 5 for  
245 the summer months. Simulated DO often overestimates observed DO, but remains  
246 typically within one standard deviation of the observations except for the bottom layer  
247 (e.g. in June).

248 Observed and simulated rates of primary production (PP) and water column respiration  
249 (WR) are shown in Figure 6, and statistical measures of model-data agreement are given  
250 in Table 2. The model simulates the observed PP reasonably well, but underestimates the  
251 WR observations, although the model is within one standard deviation of the observations  
252 (Fig. 6 and Table 2).

253 Simulated SOC within all 4 regions is plotted against bottom DO and compared with  
254 available observations in Figure 7. Simulated SOC increases with increasing bottom DO  
255 for oxygen concentrations below  $\sim 80 \text{ mmol O}_2 \text{ m}^{-3}$  and declines thereafter because of the  
256 temperature effect (SOC halves for each temperature decrease of  $10 \text{ }^\circ\text{C}$ ). SOC  
257 observations from different sources vary over a large range from 0 to  $40 \text{ mmol O}_2 \text{ m}^{-2} \text{ d}^{-1}$   
258 (Fig. 7). **Simulated SOC is at the upper range of the available observations.** Model bias in  
259 Table 3 indicates that the median of simulated SOC overestimates the observed SOC  
260 when combining all sources (average bias  $18.2 \text{ mmol O}_2 \text{ m}^{-2} \text{ d}^{-1}$ ).

### 261 **3.2 Validation of the Model+CCR simulation**

262 The model biases described in previous section (i.e. the underestimation of WR and  
263 overestimation of SOC) motivated us to carry out an additional simulation (Model+CCR)  
264 with increased WR. The additional, constant oxygen consumption rate ( $1.5 \text{ mmol O}_2 \text{ m}^{-3}$   
265  $\text{d}^{-1}$ ) was determined from Table 2 (average bias of  $30.8 \text{ mmol O}_2 \text{ m}^{-2} \text{ d}^{-1}$  divided by the  
266 average water column depth of  $20.4 \text{ m}$ ) and should compensate for the bias in model-  
267 simulated WR.

268 Compared with the previous model simulation, Model+CCR reduces the overall model  
269 data discrepancy in WR (average bias of  $-1.0 \text{ mmol O}_2 \text{ m}^{-2} \text{ d}^{-1}$ ) but overestimates the  
270 observed WR in the Mid-shelf region (bias of  $35.6 \text{ mmol O}_2 \text{ m}^{-2} \text{ d}^{-1}$ ) (Fig. 6 and Table 2).  
271 The increased WR draws down the simulated DO concentrations, improving agreement  
272 between the observed and simulated bottom DO in all regions (average bias of  $9.1 \text{ mmol}$   
273  $\text{O}_2 \text{ m}^{-3}$ ) except in the Mid-shelf region where the observed bottom DO is significantly  
274 underestimated (bias of  $-18.8 \text{ mmol O}_2 \text{ m}^{-3}$ ) (Fig. 4 and Table 1). Compared to the  
275 previous simulation, the reduced DO concentrations throughout the water column in

276 Model+CCR generally improve the model performance with lower biases, except for the  
277 Mid-shelf region in June and July (Fig. 5). The reduced bottom DO concentrations in  
278 Model+CCR also lead to a reduction in the simulated SOC (as SOC is dependent on  
279 bottom DO) and thereby slightly improve the agreement between simulated and observed  
280 SOC with lower RMSE and bias (average bias of  $14.9 \text{ mmol O}_2 \text{ m}^{-2} \text{ d}^{-1}$ ) (Fig. 7 and Table  
281 3).

### 282 **3.3 Oxygen balance**

283 In this section, we evaluate the DO balance for the summer period (June to August) for  
284 different regions of the LA shelf to identify the key processes controlling hypoxia. We  
285 focus the detailed analysis on the model simulation without additional WR; results from  
286 Model+CCR will be discussed at the end of the section. For simplicity, we are  
287 considering that oxygen consumption due to nitrification to be included in the respiration  
288 term, and not as a separate process for deriving the oxygen balance. Though we are  
289 referring to the sum of respiration and nitrification as WR, we recognize that nitrification  
290 is a chemoautotrophic process. While not strictly accurate, this is consistent with the use  
291 of WR in the observational literature where measurements of water column oxygen  
292 consumption include the contribution of nitrification.

293 We first explore the simulated seasonal and spatial patterns in water column  
294 metabolism across the shelf and its interaction with the air-sea flux of oxygen (Fig. 8).  
295 The Mississippi Delta and Atchafalaya Plume regions, which are directly impacted by the  
296 river, transit from autotrophy in June and July to heterotrophy for the rest of the year. The  
297 Mississippi Intermediate and Mid-shelf regions, however, are heterotrophic throughout  
298 the year. In terms of air-sea exchange, oxygen is outgassing during summer and taken up

299 during the rest of the year in all sub-regions, corresponding to the seasonal pattern in  
300 water column metabolism (more heterotrophic in winter and less heterotrophic or  
301 autotrophic in summer) and the seasonal cycle of surface water temperatures, which  
302 affect oxygen solubility contributing to outgassing in summer and uptake in winter. The  
303 oxygen flux into the ocean increases with the degree of heterotrophy, demonstrating the  
304 important role of air-sea gas exchange in replenishing DO in the water column.

305 When considering an oxygen balance for the water column it is useful to distinguish  
306 distinct vertical layers. We considered the following three layers in our analysis of the  
307 summer oxygen balance: a surface layer above the main pycnocline, a mid-layer  
308 extending from the main pycnocline to 5 m above the sediment and a 5-m thick bottom  
309 layer above the sediment (i.e., the layer where hypoxia occurs most frequently, as  
310 demonstrated in Figure 6 in Fennel et al., 2013). We defined the pycnocline as the depth  
311 of maximum Brunt-Vaisala Frequency (Pond and Pickard, 1983) and restricted our  
312 analysis to horizontal grid cells where all three layers existed (i.e. a main pycnocline was  
313 present and was more than 5 m above the bottom). We then integrated the terms in Eq. (1)  
314 vertically over each layer at each desired grid cell on each desired day. The advection and  
315 diffusion terms were evaluated as divergences, namely fluxes of DO into or out of the  
316 given volume through advection or diffusion. Finally we averaged the integrated results  
317 over all grid cells within a selected sub-region and over June to August in order to obtain  
318 the summer oxygen balance for the sub-regions.

319 Figure 9 shows the summer oxygen balance in the three layers and four sub-regions  
320 (numbers are provided in Table S2 of the Online Supplement). The surface layers in all  
321 four sub-regions are autotrophic while the bottom layers are heterotrophic (Fig. 9). In the

322 surface layer, biochemical processes (PP and WR) far exceed physical transport of  
323 oxygen. The positive net community production and decreasing oxygen solubility  
324 associated with the increasing water temperature in summer lead to oxygen outgassing to  
325 the atmosphere and net transport of oxygen downward to deeper waters.

326 The mid-layer is autotrophic in all four sub-regions as well, with an average PP of 48%  
327 occurring below the pycnocline and 38% in the mid-layer. About 10% of PP occurs  
328 within the 5-m bottom layer where hypoxia occurs most frequently (Fig. 9). We  
329 compared the simulation results with observations from Lehrter et al. (2009), as  
330 percentage of production below the pycnocline for each cruise (Table 4). Considering the  
331 rather large observed standard deviations, the percentages of sub-pycnocline PP in the  
332 simulations (18.6 - 40.9%) agree well with observations (23.3 - 38.7%).

333 On average the sub-pycnocline PP offsets 68% of total respiration below the pycnocline  
334 and 27% of total respiration within the 5-m bottom layer (Fig. 9). The percentages are  
335 higher in 2006 (a drought year) where PP offsets 72% of total respiration below  
336 pycnocline and 31% of total respiration within the bottom 5 m.

337 The 5-m bottom layer is heterotrophic in all sub-regions with SOC representing the  
338 single largest oxygen flux (Fig. 9). The SOC accounts for 36% of total respiratory  
339 oxygen demand below the pycnocline when averaged over the shelf and summer months.  
340 The fraction of SOC rises to 68% when limited to the bottom 5 m (Fig. 9). Driven by the  
341 strong vertical DO gradient in the water column, vertical diffusion is the primary mode of  
342 DO replenishment for the bottom layer offsetting on average 32% of total respiration over  
343 the shelf. Advection, driven by the typical summer upwelling circulation on the LA shelf,

344 is another important DO source for bottom waters offsetting on average 29% of total  
345 respiration shelf-wide.

346 Adding WR in the Model+CCR simulation impacted the summer oxygen balance by  
347 making the water column more heterotrophic and decreasing the relative contributions of  
348 SOC and WR to total respiration (Table S3 and Fig. S3). In Model+CCR the mid layers  
349 in all sub-regions and all three layers in Mid-shelf region become heterotrophic in  
350 summer months. Also, the simulated fraction of SOC to total respiration averaged over  
351 the 4 sub-regions during summer decreases from 36% to 26% within below-pycnocline  
352 water layer and from 68% to 57% within the bottom 5-m layer.

### 353 **3.4 Role of sub-pycnocline PP in hypoxia generation**

354 Time series of simulated hypoxic area from the sensitivity run without biological  
355 processes in the water column (Model w/o PP and WR) are shown in comparison to the  
356 full model and the observed hypoxic extent in Figure 10. The temporal evolution of  
357 hypoxic area is almost identical in both simulations, with ‘Model w/o PP and WR’  
358 simulating an only slightly larger hypoxic area in summer. A similar pattern is observed  
359 for simulated hypoxic volume (Fig. S1) and for the simulations with the additional  
360 oxygen sink (Fig. S4).

361

## 362 **4. Discussion**

### 363 **4.1 Simulated oxygen dynamics and model validation**

364 Overall, the model simulates the evolution of oxygen and the magnitudes and spatial  
365 distribution of PP well, but tends to overestimate bottom DO and underestimate WR

366 (within one standard deviation of observations). One possible explanation is that the  
367 model does not receive any dissolved or particulate organic matter inputs from estuarine  
368 sources other than the Mississippi and Atchafalaya rivers. Several recent studies (Bianchi  
369 et al. 2010, Murrell et al. 2013a, and Fry et al. 2014) suggested that the inshore coastal  
370 waters represent a source of oxygen-consuming organic matter that may be episodically  
371 transported onto the LA shelf.

372 The model also overestimates the observed SOC from all sources, especially those  
373 observed by Lehrter et al. (2012) and Murrell and Lehrter (2011) (Fig. 7, Table 3). Using  
374 the same model as in this study, Fennel et al. (2013) have shown that generation of  
375 hypoxia on the LA shelf is very sensitive to the parameterization of SOC, primarily  
376 because the hypoxic conditions on the shelf are restricted to a relatively thin layer above  
377 the sediment. Fennel et al. (2013) have further shown that the SOC parameterization  
378 based on observations from Rowe et al. (2002), which is used in this study, performed  
379 best in simulating the observed hypoxic extent whereas parameterization based on lower  
380 SOC values from Murrell and Lehrter (2011) led to almost no hypoxia in this model. The  
381 apparent discrepancy between SOC observations and parameterizations used in  
382 mechanistic models remains to be reconciled. One explanation could be that empirical  
383 SOC measurements underestimate the true oxygen demand, because they do not account  
384 for accumulation of reduced metabolites of anaerobic metabolism (e.g.,  $\text{NH}_4^+$ ,  $\text{HS}^-$ ,  $\text{Fe}^{2+}$ ).  
385 Accumulation of anaerobic metabolites can be episodically important in scavenging  
386 oxygen, thus acting to maintain hypoxic conditions during periods when traditional SOC  
387 measurements suggest a small DO sink. This interpretation is supported by Lehrter et al.  
388 (2012) who found that DIC fluxes (a better measure of total oxygen demand) were

389 relatively constant and insensitive to overlying DO concentration. Another explanation  
390 could be that the thickness of the simulated bottom boundary layer is overestimated. If  
391 this is the case, SOC would have to be larger than in reality in order to produce hypoxic  
392 bottom water. Future work on validating the expression and dynamics of the bottom  
393 boundary layer and its effect on hypoxia dynamics will address this question.

394 The SOC parameterization has the inherent limitation that it does not account for spatial  
395 variability in the supply of particulate organic matter reaching the sediment. An  
396 alternative model, where SOC varies responsive to the amount of organic matter sinking  
397 to the sediment (Fennel et al. 2011, 2013), essentially simulated identical results as  
398 presented here. While the SOC parameterization used here is simple, it does include two  
399 key parameters known to modulate SOC: temperature and dissolved oxygen.

400 In order to assess the effects of the model biases in WR we conducted a sensitivity  
401 experiment where an additional, constant oxygen consumption rate was applied to the  
402 water column DO based on observed WR rates from Murrell et al. (2013a). This  
403 generally improves the comparisons among measured and simulated WR, bottom water  
404 DO and SOC except in the Mid-shelf region where WR is overestimated and bottom DO  
405 is underestimated. The increased WR and slightly decreased SOC in the Model+CCR  
406 simulation also reduce the SOC fraction of total respiratory oxygen demand.

#### 407 **4.2. Primary processes controlling oxygen dynamics**

408 The simulated seasonal transition from autotrophy to heterotrophy in the Mississippi  
409 Delta and Atchafalaya Plume regions has previously been reported in mesohaline waters  
410 (salinity: 15-29) in the Mississippi River plume (Breed et al., 2004). The Mississippi  
411 Intermediate and Mid-shelf regions were heterotrophic throughout the year, implying a

412 net import of organic carbon. This result is consistent with the observations of Murrell et  
413 al. (2013a) who found net heterotrophy on the western shelf and in deeper waters of the  
414 LA shelf. A more recent study by Fry et al. (2014) also suggested that the autotrophic  
415 near-river and nearshore areas could be net source regions of carbon fueling hypoxia in  
416 adjacent mid-shelf waters.

417 Despite the heterotrophy, the main sink for oxygen is outgassing in the Mississippi  
418 Intermediate and Mid-shelf regions during the summer hypoxic season. This result is  
419 consistent with frequent observations of supersaturated DO concentrations in surface  
420 plume waters, particularly in the Louisiana Bight region (Murrell et al. 2013b). The  
421 simultaneous occurrence of heterotrophy and outgassing of oxygen is primarily due to  
422 density stratification of the water column, which isolates the autotrophic upper waters  
423 that actively exchange oxygen with the atmosphere from the heterotrophic waters below.  
424 As shown in the summer DO balance (Fig. 9), the surface layers above the pycnocline  
425 were autotrophic in all sub-regions, driving outgassing of oxygen to the atmosphere  
426 despite the whole water column being heterotrophic. The decreased oxygen solubility of  
427 warmer waters typical of summer conditions also promotes outgassing, but the effect is  
428 relatively small compared to the autotrophy in surface waters (oxygen gas-exchange is  
429 fast and the summer change in water temperature is relatively small on the LA shelf). We  
430 have carried out sensitivity experiments where we doubled and halved the air-sea gas  
431 exchange coefficient (results not presented in the manuscript) and found that the model  
432 results are insensitive to the air-sea gas exchange rates, likely because the air-sea oxygen  
433 flux is fast.

434 It has previously been demonstrated, based on observations, that a strong near-surface  
435 pycnocline is a prerequisite for hypoxia on the LA shelf, while a weaker, near-bottom  
436 pycnocline determines the hypoxic layer that actually forms (Wiseman et al., 1997). This  
437 was confirmed by model simulations (Fennel et al., 2013), which show that hypoxia is  
438 constrained to a thin layer above the sediment over large parts of the shelf. A more recent  
439 retrospective analysis of data collected during shelf-wide sampling cruises reported that  
440 the 27-year (1985-2011) average thickness of the bottom hypoxic layer is 3.9 m and that  
441 there was an increasing trend in hypoxic layer thickness from 1985 to 2011 (Obenour et  
442 al., 2013).

443 Consistent with observations by Lehrter et al. (2009), our model demonstrated that a  
444 large fraction of PP occurred below the pycnocline and even within bottom 5-m water  
445 (Fig. 9, Table 4). This is presumably because the euphotic zone extends well below the  
446 pycnocline and sometimes to the bottom on the LA shelf (Chen et al., 2000; Lehrter et al.,  
447 2009). Lehrter et al. (2009) also observed that the euphotic zone in non-plume areas  
448 (salinity>31) is deeper than in plume areas, and that the average shelf-wide light  
449 attenuation strongly correlates with freshwater discharge from the Mississippi and  
450 Atchafalaya rivers. In agreement with these observations, the simulated percentage of  
451 sub-pycnocline PP is higher in the Mississippi Intermediate region (52% below the  
452 pycnocline and 13.6% in the 5-m bottom layer) than in the Delta region (48% and 8.3%,  
453 respectively), and higher throughout the shelf in 2006 (a drought year with low  
454 freshwater discharge) than in average over the 4 years simulated (52% compared to 48%).

455 The importance of physical transport in replenishing bottom-water DO pools has been  
456 found in other coastal systems with seasonal hypoxia including Chesapeake Bay, where

457 Kemp et al. (1992) estimated that in summer the vertical oxygen flux across the  
458 pycnocline and the net longitudinal oxygen exchange offset ~55% and ~38% of total  
459 respiration below the pycnocline, respectively. More recent modeling work by Li et al.  
460 (2015) estimated that vertical diffusion and net advective fluxes respectively offset ~27%  
461 and ~64% of total respiration in the bottom 10 m during summer. Kemp et al. (1992) also  
462 showed that increased biological consumption of DO in bottom waters of Chesapeake  
463 Bay increases horizontal and vertical DO gradients and thereby increases physical  
464 transport of DO to the bottom waters during March to July. On the LA shelf the  
465 occasional occurrence of tropical storms and hurricanes can rapidly erode stratification  
466 and replenish bottom waters with DO. The lateral advection of oxygenated water from  
467 adjacent deep basins during upwelling-favorable wind conditions can also increase  
468 bottom-water DO on the LA shelf (Rabalais et al, 2007).

469 The result that SOC is the dominant oxygen sink in waters directly overlying the  
470 sediments (within 5 m above the bottom) is consistent with previous observational  
471 estimates for the LA shelf. Quinones-Rivera et al. (2007) estimated that SOC accounts for  
472 ~73% of the total DO loss within 1 m of the sediments during summer based on  $\delta^{18}\text{O}$   
473 measurements and an isotope fractionation model. Since the isotope approach only  
474 provides relative fractions of sediment and water column respiration, we cannot directly  
475 compare SOC and WR from Quinones-Rivera et al. (2007) to our simulations. However,  
476 the simulated proportions of sediment respiration to total respiration (on average 36%  
477 below pycnocline and 68% in the 5-m bottom layer) are consistent with the estimates of  
478 Quinones-Rivera et al. (2007). Adding the additional DO sink decreased the proportions  
479 of SOC to total respiration (26% below the pycnocline and 57% in the 5-m bottom layer)

480 but did not change the model result that SOC is the dominant DO sink in the bottom 5 m,  
481 demonstrating the relative sensitivity of the model to the SOC parameterization used.

### 482 **4.3 Role of sub-pycnocline PP in hypoxia generation**

483 The [summer oxygen balance](#) presented in the previous section suggests that physical  
484 transport processes and sediment respiration are major drivers of oxygen dynamics on the  
485 LA shelf, and that PP below the pycnocline may mitigate hypoxic conditions. However,  
486 in a sensitivity experiment where we disabled all biological processes in the water  
487 column the spatial extent of hypoxic bottom waters is only slightly reduced, suggesting  
488 that PP below the pycnocline has only a minor effect on hypoxia.

489

## 490 **5. Summary and conclusions**

491 In this study we used a physical-biogeochemical model to investigate the dynamics of  
492 dissolved oxygen and hypoxia on the LA shelf and to identify the key controlling  
493 processes. Comparisons with observations demonstrate that the model simulates the  
494 evolution of oxygen well but tends to overestimate bottom DO and SOC, and  
495 underestimates WR. When adding a constant oxygen consumption rate in the water  
496 column to correct the bias in WR rates, the model-simulated oxygen dynamics agree  
497 better with observations in all sub-regions except the Mid-shelf. This result suggests that  
498 organic matter from inshore waters may need to be included in future versions of the  
499 model.

500 Consistent with observations of Murrell et al. (2013a), our model demonstrated that the  
501 LA shelf is essentially heterotrophic throughout the year except for the areas directly

502 impacted by rivers during June and July. This implies a net import of organic carbon on  
503 the LA shelf. Air-sea gas exchange was the primary mode of replenishing the very  
504 heterotrophic waters in non-summer months with relatively strong mixing. However, in  
505 summer, stratification isolates the autotrophic surface from the heterotrophic lower  
506 waters. In the Mississippi Intermediate and Mid-shelf regions this isolation results in  
507 significant outgassing of oxygen across the air-sea interface despite a heterotrophic water  
508 column, exacerbating the risk of hypoxia in these regions.

509 In summer, the model indicates that a substantial fraction of primary production  
510 (~48%) occurs below the pycnocline and about 10% of primary production occurs within  
511 5 m of the bottom where hypoxia forms most frequently. [In a sensitivity experiment](#)  
512 [where biological processes in the water column \(i.e. PP and WR\) were turned off we](#)  
513 [demonstrate that the below-pycnocline PP mitigates hypoxia only slightly, and that](#)  
514 [physical processes and sediment oxygen consumption together largely determine the](#)  
515 [spatial extent and dynamics of hypoxia on the LA shelf.](#)

516

## 517 **Acknowledgements**

518 This work was supported by NOAA CSCOR grants NA06N0S4780198 and the US IOOS  
519 Coastal Ocean Modeling Testbed. NOAA NGOMEX publication no. XXX.

520

## 521 **References**

522 Bianchi, T.S., DiMarco, S.F., Cowan Jr, J.H., Hetland, R.D., Chapman, P., Day, J.W., and  
523 Allison, M.A.: The science of hypoxia in the Northern Gulf of Mexico: A review,

524 Sci. Total Environ., 408, 1471-1484, 2010.

525 Bierman, V.J., Hinz, S.C., Zhu, D.W., Wiseman, W.J. Jr, Rabalais, N.N., and Turner, R.E.:  
526 Preliminary mass balance model of primary productivity and dissolved oxygen in the  
527 Mississippi River plume/inner gulf shelf region, Estuar., 17, 886-899, 1994.

528 Boyer, T. P., Antonov, J.I., Garcia, H.E., Johnson, D.R., Locarnini, R.A., Mishonov, A.V.,  
529 Pitcher, M.T., Baranova, O.K., and Smolyar, I.V.: World Ocean Database 2005,  
530 edited by: Levitus, S., NOAA Atlas NESDIS 60, US Government Printing Office,  
531 Washington, DC, 190 pp., DVDs, 2006.

532 Breed, G.A., Jackson, G.A., and Richardson T.L.: Sedimentation, carbon export and food  
533 web structure in the Mississippi River plume described by inverse analysis, Mar.  
534 Ecol. Prog. Ser., 278, 35-51, 2004.

535 Cerco, C.F.: Response of Chesapeake Bay to nutrient load reductions, J. Environ. Eng.,  
536 121(8), 549-557, 1995.

537 Cerco, C.F. and Cole, T.M.: Three-dimensional eutrophication model of Chesapeake Bay,  
538 J. Environ. Eng., 119(6), 1006-1025, 1993.

539 Chen, X., Lohrenz, S.E., and Wiesenburg, D.A.: Distribution and controlling mechanisms  
540 of primary production on the Louisiana-Texas continental shelf, J. Mar. Syst., 25,  
541 179-207, 2000.

542 Cho, K., Reid, R.O., and Nowlin, W.D.: Objectively mapped stream function fields on the  
543 Texas–Louisiana shelf based on 32 months of moored current meter data, J. Geophys.  
544 Res., 103 (C5), 10377-10390, 1998.

545 Cochrane, J.D. and Kelly, F.J.: Low-frequency circulation on the Texas-Louisiana  
546 continental shelf, J. Geophys. Res., 91 (C9), 10645-10659, 1986.

547 da Silva, A.M., Young-Molling, C.C., and Levitus, S.: Atlas of Surface Marine Data 1994  
548 Vol. 3, Anomalies of fluxes of heat and momentum. NOAA Atlas NESDIS 8, Natl.  
549 Oceanic and Atmos. Admin., Silver Spring, MD, 1994a.

550 da Silva, A.M., Young-Molling, C.C., and Levitus, S.: Atlas of Surface Marine Data 1994  
551 Vol. 4, Anomalies of fresh water fluxes, NOAA Atlas NESDIS 9, Natl. Oceanic and  
552 Atmos. Admin., Silver Spring, MD, 1994b.

553 Eldridge, P.M. and Morse, J.W.: Origins and temporal scales of hypoxia on the Louisiana  
554 shelf: Importance of benthic and sub-pycnocline water metabolism. *Mar. Chem.*,  
555 108, 159-171, 2008.

556 Eldridge, P.M. and Roelke, D.L.: Origins and scales of hypoxia on the Louisiana shelf:  
557 importance of seasonal plankton dynamics and river nutrients and discharge. *Ecol.*  
558 *Model.*, 221, 1028-1042, 2010.

559 Feng, Y., DiMarco, S.F., and Jackson, G.A.: Relative role of wind forcing and riverine  
560 nutrient input on the extent of hypoxia in the northern Gulf of Mexico, *Geophys.*  
561 *Res. Lett.*, 39, L09601, doi:10.1029/2012GL051192, 2012.

562 Feng, Y., Fennel, K., Jackson, G.A., DiMarco, S.F., and Hetland, R.D.: A model study of  
563 the response of hypoxia to upwelling-favorable wind on the northern Gulf of Mexico  
564 shelf, *J. Mar. Syst.*, 131, 63-73, 2014.

565 Fennel, K., Wilkin, J., Levin, J., Moisan, J., O'Reilly, J., and Haidvogel, D.: Nitrogen  
566 cycling in the Middle Atlantic Bight: results from a three-dimensional model and  
567 implications for the North Atlantic nitrogen budget, *Global Biogeochem. Cy.*, 20,  
568 GB3007, doi:10.1029/2005GB002456, 2006.

569 Fennel, K., Hetland, R.D., Feng, Y., and DiMarco, S.: A coupled physical-biological

570 model of the Northern Gulf of Mexico shelf: model description, validation and  
571 analysis of phytoplankton variability, *Biogeosciences*, 8, 1881-1899, 2011.

572 Fennel, K., Hu, J., Laurent, A., Marta-Almeida, M., and Hetland, R.D.: Sensitivity of  
573 hypoxia predictions for the Northern Gulf of Mexico to sediment oxygen  
574 consumption and model nesting, *J. Geophys. Res.*, 118, 990-1002, 2013.

575 [Flather, R. A.: A tidal model of the northwest European continental shelf, \*Memoires de la\*](#)  
576 [Societe Royale de Sciences de Liege, 141-164, 1976.](#)

577 Forrest, D., Hetland, R.D., and DiMarco, S.: Multivariable statistical regression models  
578 of the areal extent of hypoxia over the Texas-Louisiana continental shelf. *Environ.*  
579 *Res. Lett.*, 6, 1-10, 2011.

580 Fry, B., Justic', D., Riekenberg, P., Swenson, E., Turner, R.E., Wang, L., Pride, L.,  
581 Rabalais, N.N., Kurtz, J.C., Lehrter, J.C., Murrell, M.C., Shadwick, E.H. and Boyd,  
582 B.: Carbon dynamics on the Louisiana continental shelf and cross-shelf feeding of  
583 hypoxia. *Estuar. Coast.*, DOI 10.1007/s12237-014-9863-9, 2014

584 Green, R.E., Breed, G.A., Dagg, M.J., and Lohrenz, S.E.: Modeling the response of  
585 primary production and sedimentation to variable nitrate loading in the Mississippi  
586 River plume, *Cont. Shelf Res.*, 28, 1451-1465, 2008.

587 Greene, R.M., Lehrter, J., and Hagy, J.: Multiple regression models for hindcasting and  
588 forecasting midsummer hypoxia in the Gulf of Mexico, *Ecol. Appl.*, 19, 1161-1175,  
589 2009.

590 Haidvogel, D. B., Arango, H., Budgell, W. P., Cornuelle, B. D., Curchitser, E., Di  
591 Lorenzo, E., Fennel, K., Geyer, W. R., Hermann, A. J., Lanerolle, L., Levin, J.,  
592 McWilliams, J. C., Miller, A. J., Moore, A. M., Powell, T. M., Shchepetkin, A. F.,

593 Sherwood, C. R., Signell, R. P., Warner, J. C., and Wilkin, J.: Ocean forecasting in  
594 terrain-following coordinates: formulation and skill assessment of the regional ocean  
595 modeling system, *J. Comput. Phys.*, 227, 3595-3624, 2008.

596 Hetland, R.D. and DiMarco, S.F.: How does the character of oxygen demand control the  
597 structure of hypoxia on the Texas-Louisiana continental shelf?, *J. Mar. Syst.*, 70, 49-  
598 62, 2008.

599 Hetland, R.D. and DiMarco, S.F.: Skill assessment of a hydrodynamic model of  
600 circulation over the Texas- Louisiana continental shelf, *Ocean Modell.*, 43/44, 64-76,  
601 2012.

602 Justić, D., Rabalais, N.N., and Turner, R.E.: Effects of climate change on hypoxia in  
603 coastal waters: a doubled CO<sub>2</sub> scenario for the northern Gulf of Mexico. *Limnol.*  
604 *Oceanogr.*, 41, 992-1003, 1996.

605 Justić, D., Rabalais, N.N., and Turner, R.E.: Modeling the impacts of decadal changes in  
606 riverine nutrient fluxes on coastal eutrophication near the Mississippi River delta,  
607 *Ecol. Model.*, 152, 33-46, 2002.

608 Justić, D. and Wang, L.: Assessing temporal and spatial variability of hypoxia over the  
609 inner Louisiana–upper Texas shelf: Application of an unstructured-grid three-  
610 dimensional coupled hydrodynamic-water quality model, *Cont. Shelf Res.*, 72, 163-  
611 179, 2014.

612 [Kemp, W.M., Sampou, P.A., Garber, J., Tuttle, J., and Boynton, W.R.: Seasonal](#)  
613 [depletion of oxygen from bottom waters of Chesapeake Bay: Roles of benthic and](#)  
614 [planktonic respiration and physical exchange processes, \*Mar. Ecol.-Prog. Ser.\*, 85,](#)  
615 [137-152, 1992.](#)

616 Laurent, A., Fennel, K., Hu, J., and Hetland, R.D.: Simulating the effects of phosphorus  
617 limitation in the Mississippi and Atchafalaya River plumes, *Biogeosciences*, 9, 4707-  
618 4723, 2012.

619 Laurent, A. and Fennel, K.: Simulated reduction of hypoxia in the northern Gulf of  
620 Mexico due to phosphorus limitation, *Elementa*, doi:10.12952/journal.elementa.  
621 000022, 2014.

622 Lehrter, J.C., Murrell, M.C., and Kurtz, J.C.: Interactions between Mississippi River  
623 inputs, light, and phytoplankton biomass and phytoplankton production on the  
624 Louisiana continental shelf, *Cont. Shelf Res.*, 29, 1861-1872, 2009.

625 Lehrter, J.C., Beddick, D.L., Devereux, R., Yates, D.F., and Murrell, M.C.: Sediment-  
626 water fluxes of dissolved inorganic carbon, O<sub>2</sub>, nutrients, and N<sub>2</sub> from the hypoxic  
627 region of the Louisiana continental shelf, *Biogeochemistry*, 109, 233-252, 2012.

628 Lehrter, J.C., Ko, D.S., Murrell, M.C., Hagy, J.D., Schaeffer, B.A., Greene, R.M., Gould,  
629 R.W., and Penta, B.: Nutrient distributions, transports, and budgets on the inner  
630 margin of a river-dominated continental shelf, *J. Geophys. Res.- Oceans*, 118, 4822-  
631 4838, 2013.

632 Lehrter, J.C., Fry, B., and Murrell, M.C.: Microphytobenthos production potential and  
633 contribution to bottom layer oxygen dynamics on the inner Louisiana continental  
634 shelf, *Bull. Mar. Sci.*, 90(3): 765-780, 2014.

635 Li, Y., Li, M., and Kemp, M.: A budget analysis of bottom-water dissolved oxygen in  
636 Chesapeake Bay, *Estuar. Coast*, DOI 10.1007/s12237-014-9928-9, 2015.

637 McCarthy, M.J., Carini, S.A., Liu, Z., Ostrom, N.E., and Gardner, W.S.: Oxygen  
638 consumption in the water column and sediments of the northern Gulf of Mexico

639 hypoxic zone., *Estuar. Coast. Shelf. Sci.*, 123, 46-53, 2013.

640 Mellor, G.L. and Yamada, T.: Development of a turbulence closure model for geophysical  
641 fluid problems. *Rev. Geophys. Space Phys.*, 20, 851-875, 1982.

642 Murrell, M.C. and Lehrter, J.C.: Sediment and lower water column oxygen consumption  
643 in the seasonally hypoxic region of the Louisiana continental shelf, *Estuar. Coasts*,  
644 34, 912-924, 2011.

645 Murrell, M.C., Stanley, R.S., and Lehrter, J.C.: Plankton community respiration, net  
646 ecosystem metabolism, and oxygen dynamics on the Louisiana continental shelf:  
647 implications for hypoxia, *Cont. Shelf Res.*, 52, 27-38, 2013a.

648 Murrell, M.C., Beddick, D.L., Devereux, R., Greene, R.M., Hagy, J.D., Jarvis, B.M.,  
649 Kurtz, J.C., Lehrter, J.C. and Yates, D.F. (2013) Gulf of Mexico hypoxia research  
650 program data report: 2002-2007, p. 217, U. S. Environmental Protection Agency,  
651 Washington, DC, EPA/600/R-13/257, <http://tinyurl.com/ko9wj7j>, 2013b

652 Nunnally, C.C., Rowe, G.T., Thornton, D.C.O., and Quigg, A.: Sediment oxygen  
653 consumption and nutrient regeneration in the Northern Gulf of Mexico Hypoxic  
654 Zone, *J. Coast. Res.*, 63, 84-96, 2013.

655 Obenour, D.R., Scavia, D., Rabalais, N.N., Turner, R.E., and Michalak, A.M.:  
656 Retrospective analysis of midsummer hypoxic area and volume in the Northern Gulf  
657 of Mexico, 1985–2011, *Environ. Sci. Technol.*, 47, 9808-9815, 2013.

658 Pond, S. and Pickard, G.L.: *Introductory dynamical oceanography*, 2nd edition Pergamon  
659 Press, Oxford. 1983.

660 Quinones-Rivera, Z.J., Wissel, B., Justic, D., and Fry, B.: Partitioning oxygen sources  
661 and sinks in a stratified, eutrophic coastal ecosystem using stable oxygen isotopes,

662 Mar. Ecol. Prog. Ser., 342, 69-83, 2007.

663 Quinones-Rivera, Z.J., Wissel, B., Rabalais, N.N., and Justic, D.: Effects of biological and  
664 physical factors on seasonal oxygen dynamics in a stratified, eutrophic coastal  
665 ecosystem, *Limnol. Oceanogr.*, 55 (1), 289-304, 2010.

666 Rabalais, N.N., Turner, R.E., and Wiseman, W.J.: Gulf of Mexico hypoxia, a.k.a. “The  
667 Dead Zone”, *Ann. Rev. Ecol. Syst.*, 33, 235-263, 2002.

668 Rabalais, N.N., Turner, R.E., Sen Gupta, B.K., Boesch, D.F., Chapman, P., and Murrell,  
669 M.C.: Hypoxia in the northern Gulf of Mexico: Does the science support the plan to  
670 reduce, mitigate, and control hypoxia?, *Estuar. Coast.*, 30, 753-772, 2007.

671 Rowe, G.T. and Chapman, P.: Continental shelf hypoxia: some nagging questions, *Gulf  
672 of Mexico Sci.*, 20, 153-160, 2002.

673 Rowe, G.T., Kaeki, M.E.C., Morse, J.W., Boland, G.S., and Briones, E.G.E.: Sediment  
674 community metabolism associated with continental shelf hypoxia, northern Gulf of  
675 Mexico, *Estuar.*, 25 (6), 1097-1106, 2002.

676 Scully, M. E.: Physical controls on hypoxia in Chesapeake Bay: A numerical modeling  
677 study, *J. Geophys. Res.*, 118, 1239-1256, 2013.

678 Shen, Y., Fichot, C.G., and Benner, R.: Floodplain influence on dissolved organic matter  
679 composition and export from the Mississippi-Atchafalaya River system to the Gulf of  
680 Mexico, *Limnol. Oceanogr.* 57 (4), 1149-1160, 2012.

681 Testa, J.M. and Kemp, W.M.: Oxygen - Dynamics and Biogeochemical Consequences.  
682 In: Wolanski, E. and McLusky, D.S. (eds.) *Treatise on Estuarine and Coastal  
683 Science*, Vol 5, 163-199, Waltham: Academic Press, 2011.

684 Turner, R., Rabalais, N., Swenson, E., Kasprzak, M., and Romaine, T.: Summer hypoxia

685 in the Northern Gulf of Mexico and its prediction from 1978 to 1995, *Mar. Environ.*  
686 *Res.*, 59, 65-77, 2005.

687 Turner, R. E., Rabalais, N. N., and Justic, D.: Predicting summer hypoxia in the northern  
688 Gulf of Mexico: Riverine N, P, and Si loading, *Mar. Pollut. Bull.*, 52, 139-148, 2006.

689 Wanninkhof, R.: Relationship between wind speed and gas exchange, *J. Geophys. Res.*,  
690 97, 7373-7382, 1992.

691 Wiseman, W., Rabalais, N., Turner, R., Dinnel, S., and MacNaughton, A.: Seasonal and  
692 interannual variability within the Louisiana coastal current: stratification and  
693 hypoxia, *J. Mar. Syst.*, 12, 237-248, 1997.

694 **Table Captions**

695 **Table 1.** RMSE and bias (both in units of  $\text{mmol O}_2 \text{ m}^{-3}$ ) between simulated and observed  
696 bottom DO concentrations. Comparisons were conducted over the simulation period from  
697 2004 to 2007 using all available observations. Bias was calculated as model minus  
698 observation. N is the number of observations available for each calculation.

699 **Table 2.** RMSE and bias (both in units of  $\text{mmol O}_2 \text{ m}^{-2} \text{ d}^{-1}$ ) between simulated and  
700 observed primary production (PP) or water column respiration (WR). Comparisons were  
701 conducted over the simulation period from 2004 to 2007 using all available observations.  
702 Bias was calculated as model minus observations. N is the number of observations for  
703 each category.

704 **Table 3.** RMSE and bias (both in units of  $\text{mmol O}_2 \text{ m}^{-2} \text{ d}^{-1}$ ) between simulated median of  
705 sediment oxygen consumption (SOC) and observed SOC. The simulation period ranged  
706 from 2004 to 2007 while observations from different sources were collected during  
707 longer period from 1991 to 2011. Bias was calculated as model median minus  
708 observation with same bottom dissolved oxygen (DO) concentration. N is the number of  
709 observations available for each category.

710 **Table 4.** Shelf-wide average observed and simulated percentage of primary production  
711 below the pycnocline ( $\text{mean} \pm \text{standard deviation}$ ). N is the number of observations.

712 **Table 1.** RMSE and bias (both in units of mmol O<sub>2</sub> m<sup>-3</sup>) between simulated and observed  
 713 bottom DO concentrations. Comparisons were conducted over the simulation period from  
 714 2004 to 2007 using all available observations. Bias was calculated as model minus  
 715 observation. N is the number of observations available for each category.

	Model		Model+CCR		N
	RMSE	Bias	RMSE	Bias	
Mississippi Delta	74.6	43.3	61.6	15.6	182
Mississippi Intermediate	72.2	40.3	61.5	18.7	845
Atchafalaya Plume	66.3	35.0	58.7	16.6	377
Mid-shelf	48.9	15.6	54.0	-18.8	435
All data	66.4	33.7	59.3	9.1	1839

716

717 **Table 2.** RMSE and bias (both in units of mmol O<sub>2</sub> m<sup>-2</sup> d<sup>-1</sup>) between simulated and  
 718 observed primary production (PP) or water column respiration (WR). Comparisons were  
 719 conducted over the simulation period from 2004 to 2007 using all available observations.  
 720 Bias was calculated as model minus observations. N is the number of observations for  
 721 each category.

	PP				WR				N
	Model		Model+CCR		Model		Model+CCR		
	RMSE	Bias	RMSE	Bias	RMSE	Bias	RMSE	Bias	
Miss. Delta	145.2	-42.3	145.5	-43.6	115.8	-49.4	104.4	-17.9	55
Miss. Inter.	94.7	10.5	95.0	9.2	93.3	-45.9	84.5	-19.4	60
Atch. Plume	114.1	12.5	114.0	11.2	62.6	-27.6	58.4	-8.2	77
Mid-shelf	91.8	50.2	91.1	48.4	75.8	-7.0	81.7	35.6	71
All data	112.0	10.8	112.0	9.3	86.5	-30.8	81.9	-1.0	263

722

723

724 **Table 3.** RMSE and bias (both in units of  $\text{mmol O}_2 \text{ m}^{-2} \text{ d}^{-1}$ ) between simulated median of  
 725 sediment oxygen consumption (SOC) and observed SOC. The simulation period ranged  
 726 from 2004 to 2007 while observations from different sources were collected during  
 727 longer period from 1991 to 2011. Bias was calculated as model median minus  
 728 observation with same bottom dissolved oxygen (DO) concentration. N is the number of  
 729 observations available for each category.

	Model		Model+CCR		N
	RMSE	Bias	RMSE	Bias	
Rowe et al. 2012	15.9	11.1	13.6	8.0	12
McCarthy et al. 2013	15.8	10.2	13.9	7.0	18
Lehrter et al. 2012	26.1	24.6	22.4	20.7	22
Murrell and Lehrter 2011	24.7	21.2	21.7	18.1	31
All data	22.3	18.2	19.5	14.9	83

730

731 **Table 4.** Shelf-wide average observed and simulated percentage of primary production  
 732 below the pycnocline (mean $\pm$ standard deviation). N is the number of observations.

Cruise	N	Percentage of PP below pycnocline (%)	
		Observation	Simulation
Mar 2005	24	23.3 $\pm$ 29.4	27.8 $\pm$ 26.9
Apr 2006	31	35.3 $\pm$ 30.0	23.4 $\pm$ 25.2
Jun 2006	54	29.3 $\pm$ 25.7	18.6 $\pm$ 19.2
Sep 2006	71	38.7 $\pm$ 25.7	39.4 $\pm$ 28.2
May 2007	64	25.8 $\pm$ 25.0	36.2 $\pm$ 29.6
Aug 2007	60	24.7 $\pm$ 23.3	40.9 $\pm$ 30.9
RMSE			42.5
Bias			2.8
N			304

733 **Figure Captions**

734 **Fig. 1.** Model grid (light grey lines) and bathymetry (in meters). The black lines delineate  
735 areas used during model analysis and are referred to as Mississippi Delta, Mississippi  
736 Intermediate, Atchafalaya Plume and Mid-shelf region in the text. The black dots are  
737 stations where primary production (Lehrter et al. 2009) and respiration rates (Murrell et  
738 al. 2013) were collected.

739 **Fig. 2.** Mississippi and Atchafalaya River freshwater discharge (upper panel) and nutrient  
740 loads (lower panel) in 2004-2007. The dash line indicates the long-term climatology  
741 (1983-2010).

742 **Fig. 3.** Schematic of the biological model.

743 **Fig. 4.** Time series of simulated and observed dissolved oxygen concentration (DO) in  
744 bottom water in the Mississippi Delta, Mississippi Intermediate, Atchafalaya Plume and  
745 Mid-shelf regions. For the simulations, the medians are shown as solid lines (Model:  
746 blue line, Model+CCR: red line), the range between the 25th and 75th percentiles as dark  
747 blue/red area and the range between the minimum and maximum value as light blue/red  
748 area. For the observations, the medians of monthly binned observations are shown as  
749 black dots, the range between the 25th and 75th percentiles as thick vertical lines and the  
750 range between minimum and maximum values as thin vertical lines. The number of  
751 observations in each monthly bin is given above each maximum value. The dashed line  
752 indicates the hypoxia criterion of  $62.5 \text{ mmol O}_2 \text{ m}^{-3}$ . Observations are from Rabalais et al.  
753 (2007), Lehrter et al. (2009, 2012), Nunnally et al. (2012), Murrell et al. (2014), and the  
754 MCH program.

755 **Fig. 5.** Vertical profiles of model bias (model minus observations,  $\text{mmol O}_2 \text{ m}^{-3}$ ) in  
756 dissolved oxygen (DO) calculated from 2004 to 2007 for June to August in the 4 sub-  
757 regions. The vertical axis is the scaled depth, where 0 corresponds to the surface and -1 to  
758 the bottom. The light grey areas represent the standard deviation in the observations.  
759 Observations are from Rabalais et al. (2007), Lehrter et al. (2009, 2012), Murrell et al.  
760 (2014), and the MCH program.

761 **Fig. 6.** Vertically integrated rates of observed and simulated primary production (upper  
762 panel) and water column respiration (lower panel) in the 4 sub-regions. The error bars  
763 indicate the standard deviation. The number of observations in each sub-region is given  
764 above the error bars.

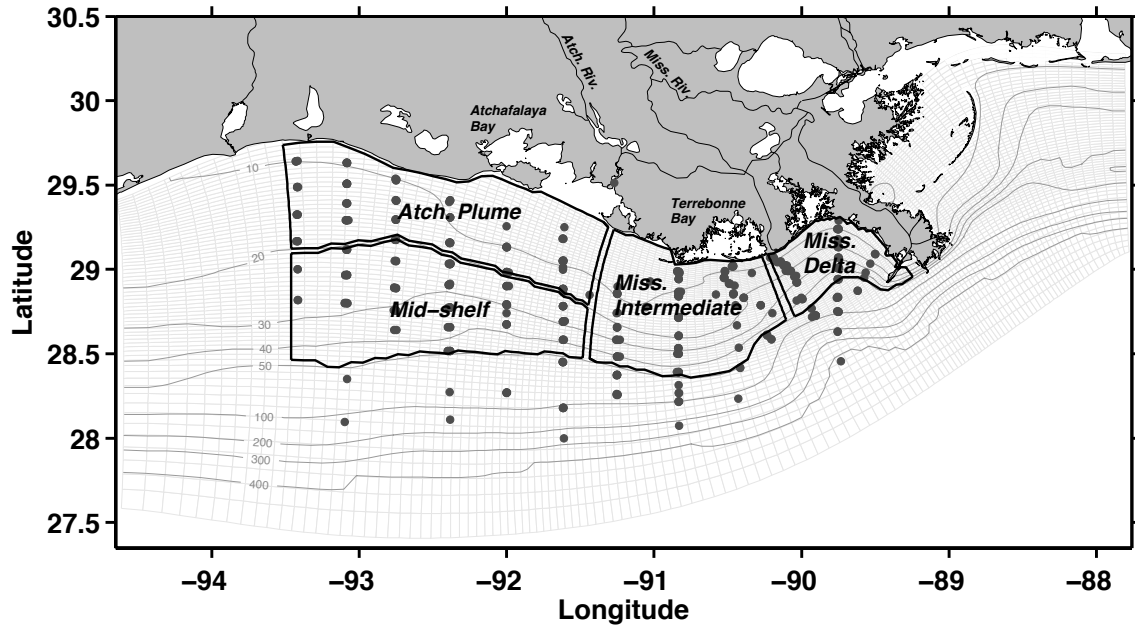
765 **Fig. 7.** Model simulated sediment oxygen consumption (SOC) versus bottom dissolved  
766 oxygen (DO) for the period 2004 to 2007, including the median (solid line) and the range  
767 between 25th and 75th percentiles (shaded area). Also shown for comparison are  
768 observations from Rowe et al. (2002), McCarthy (2013), Lehrter et al. (2012) and Murrell  
769 and Lehrter (2011).

770 **Fig. 8.** Simulated net community production (PP-TR) versus air-sea flux of oxygen for  
771 the 4 sub-regions. The colored dots represent monthly means averaged over 2004 to  
772 2007. Positive air-sea flux indicates oxygen is taken by water whereas negative air-sea  
773 flux indicates oxygen outgasses. Positive (PP-TR) suggests autotrophic whereas negative  
774 (PP-TR) suggests heterotrophic. Standard deviations of the air-sea flux in different  
775 months and sub-regions range widely from 13 to  $58 \text{ mmol O}_2 \text{ m}^{-2} \text{ d}^{-1}$  and standard  
776 deviation of (PP-TR) range from 12 to  $63 \text{ mmol O}_2 \text{ m}^{-2} \text{ d}^{-1}$ , both of which are higher in  
777 Mississippi Delta and Atchafalaya Plume and lower in the other two regions.

778 **Fig. 9.** Simulated 4-year (2004-2007) mean oxygen balance in summer for the 4 sub-  
779 regions. Oxygen source and sink terms are given for the surface layer above the  
780 pycnocline, for the mid layer and for the 5-m thick bottom layer. The average depth of  
781 the pycnocline, depth at 5 m above bottom and the average water column depth are  
782 indicated for each sub-region. The open circles indicate the balance of primary  
783 production (PP) and respiration+nitrification (WR) in each layer. For the bottom layer,  
784 the bars for respiration+nitrification (WR) and sediment oxygen consumption (SOC) are  
785 shown stacked and SOC is repeated separately. The net rate of oxygen change in each  
786 layer (i.e. the sum of all oxygen source and sink terms) is given and denoted as Net.

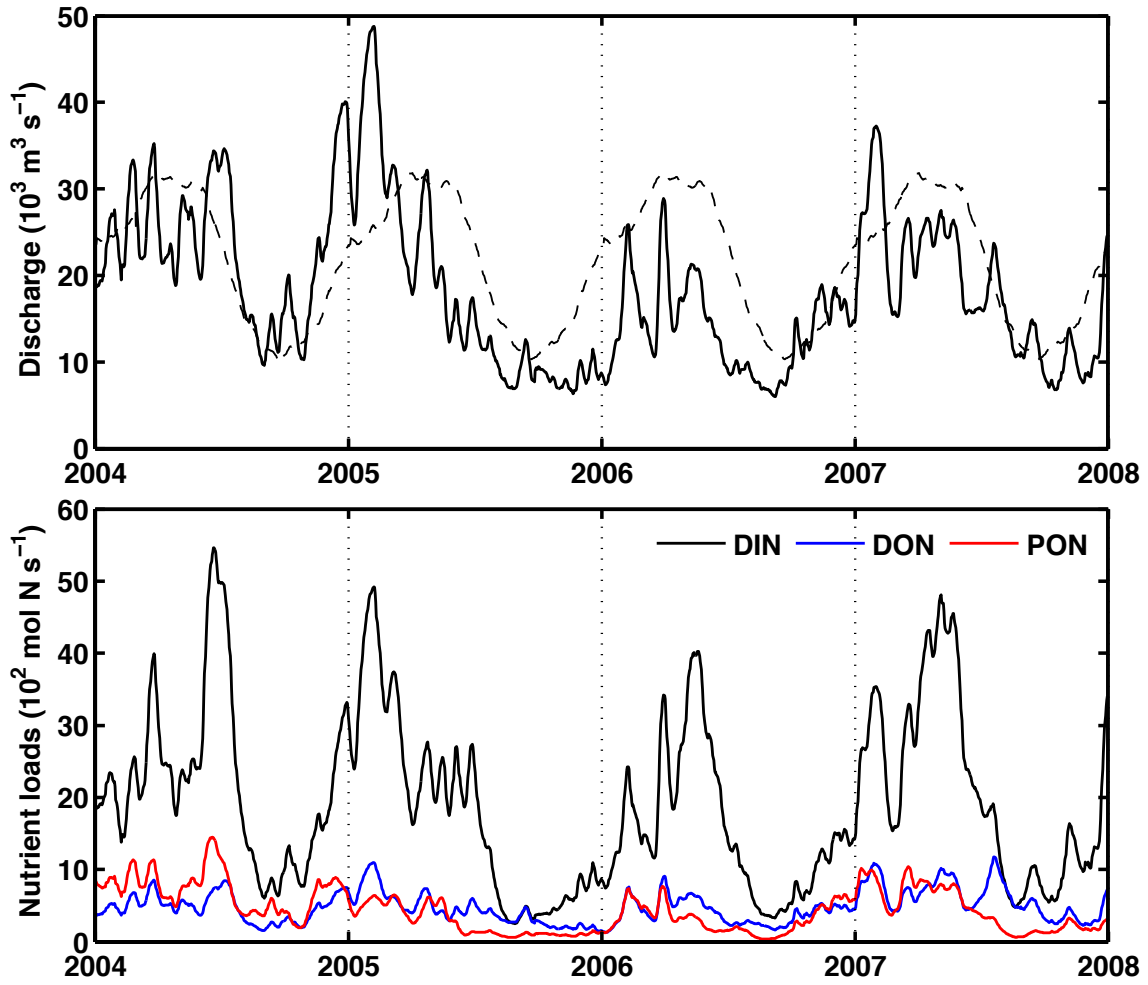
787 **Fig. 10.** Time series of simulated hypoxic extent for the full model (black line) and the  
788 model without biological processes in the water column (red line). Also shown is the  
789 observed hypoxic extent in late July (black dots). The observed hypoxic extent was  
790 estimated by linearly interpolating the observed oxygen concentrations onto the model  
791 grid and then calculating the area with oxygen concentrations below the hypoxic  
792 threshold (Fennel et al., 2013).

793



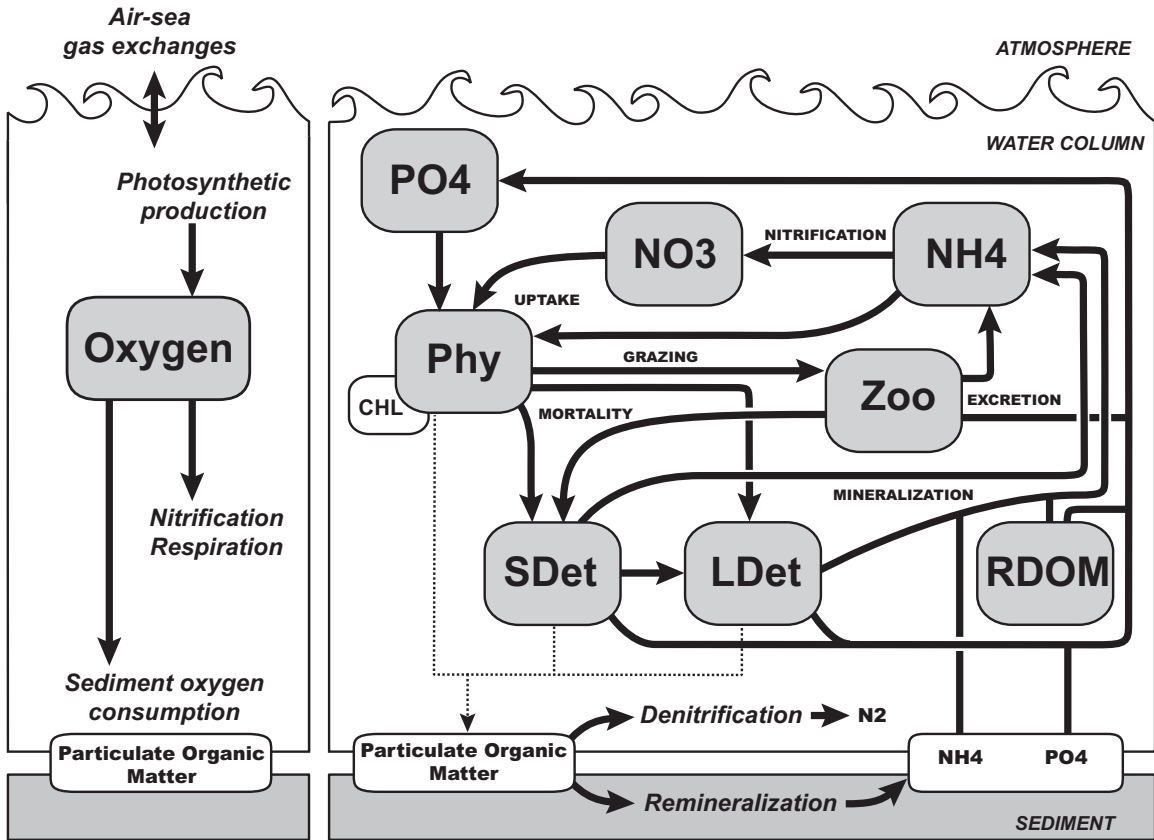
794  
795

**Fig. 1.** Model grid (light grey lines) and bathymetry (in meters). The black lines delineate areas used during model analysis and are referred to as Mississippi Delta, Mississippi Intermediate, Atchafalaya Plume and Mid-shelf region in the text. The black dots are stations where primary production (Lehrter et al. 2009) and respiration rates (Murrell et al. 2013) were collected.



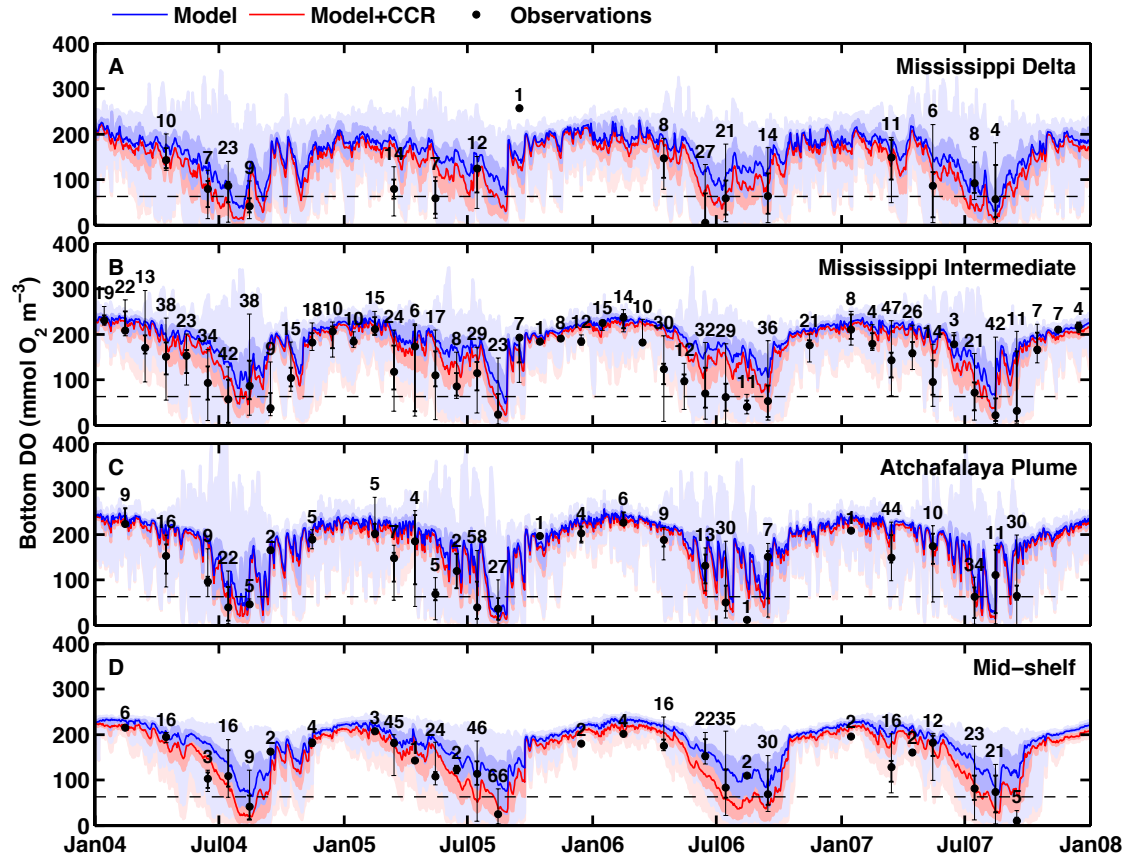
800

801 **Fig. 2.** Mississippi and Atchafalaya River freshwater discharge (upper panel) and nutrient  
 802 loads (lower panel) in 2004-2007. The dash line indicates the long-term climatology  
 803 (1983-2010).



804

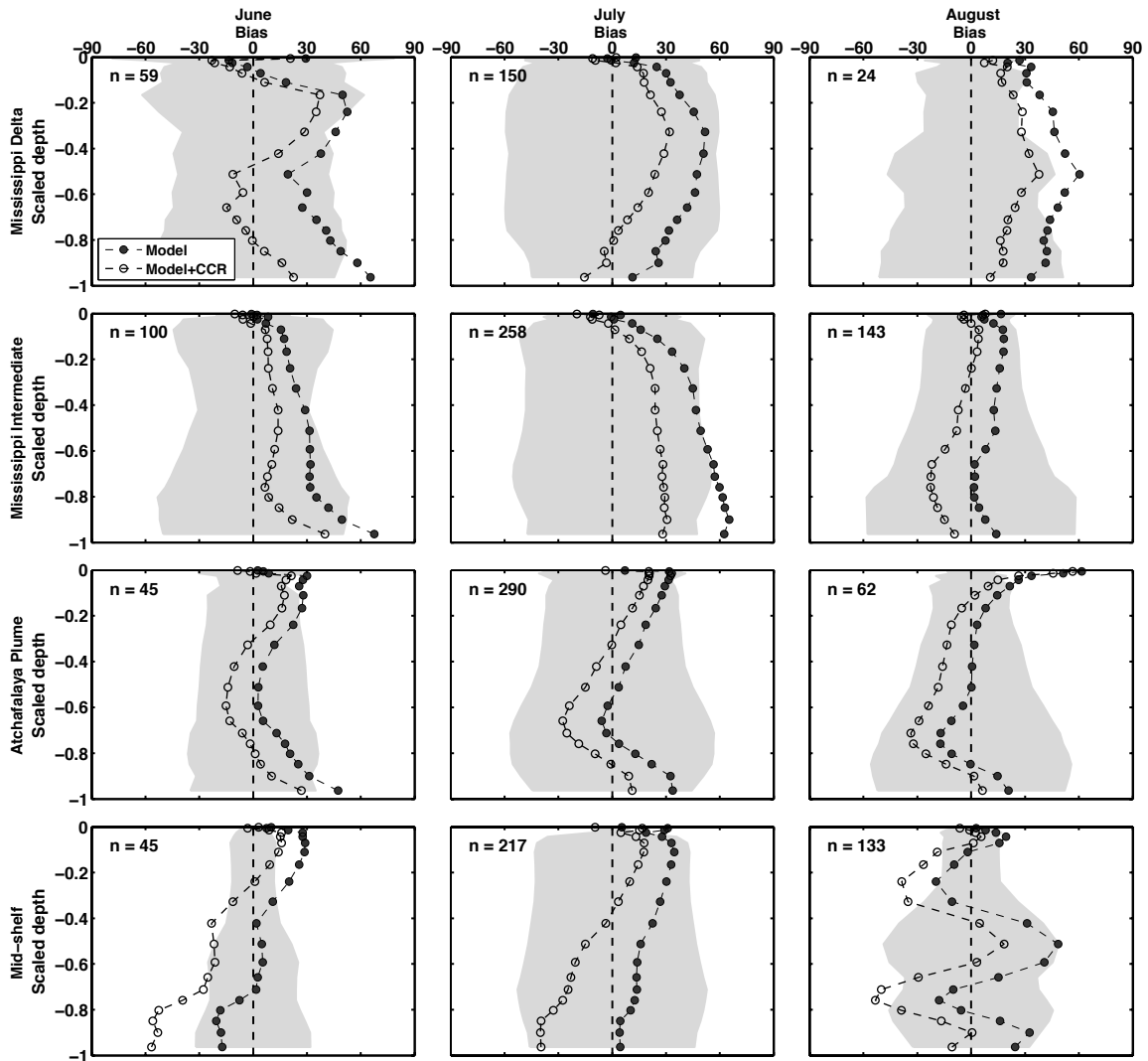
805 **Fig. 3.** Schematic of the biological model.



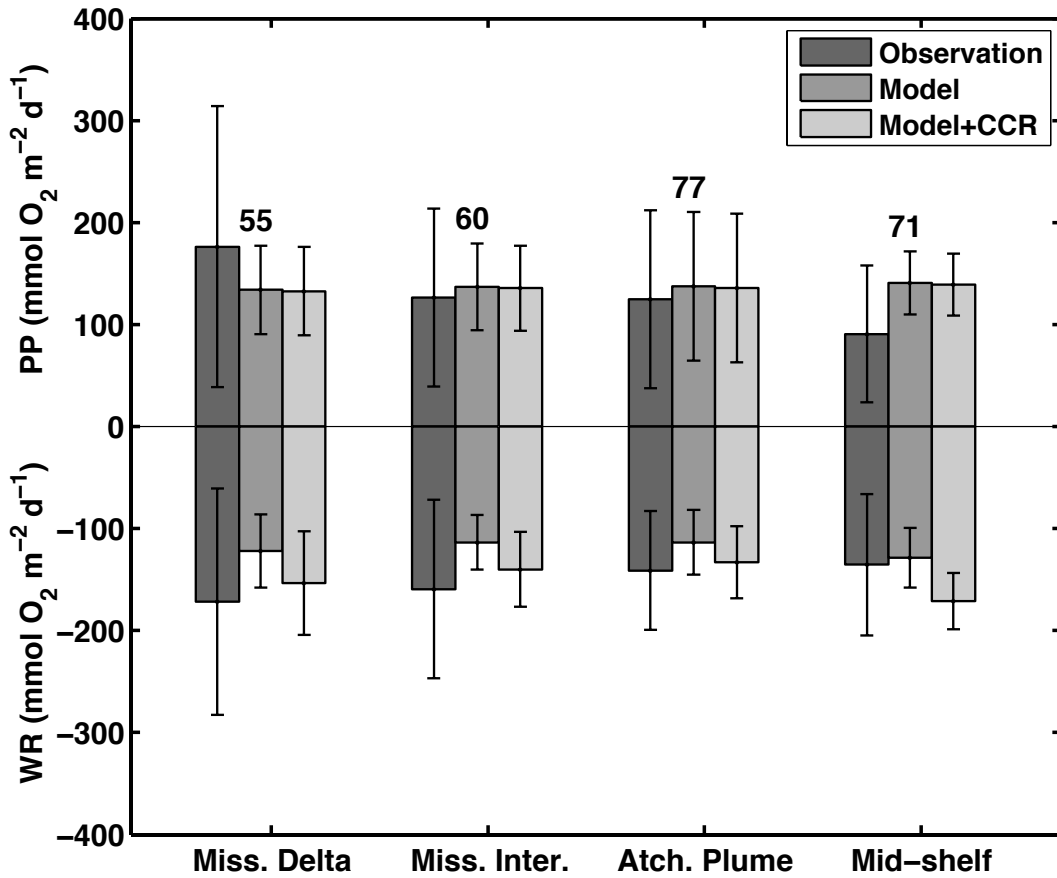
806

807 **Fig. 4.** Time series of simulated and observed dissolved oxygen concentration (DO) in  
 808 bottom water in the Mississippi Delta, Mississippi Intermediate, Atchafalaya Plume and  
 809 Mid-shelf regions. For the simulations, the medians are shown as solid lines (Model:  
 810 blue line, Model+CCR: red line), the range between the 25th and 75th percentiles as dark  
 811 blue/red area and the range between the minimum and maximum value as light blue/red  
 812 area. For the observations, the medians of monthly binned observations are shown as  
 813 black dots, the range between the 25th and 75th percentiles as thick vertical lines and the  
 814 range between minimum and maximum values as thin vertical lines. The number of  
 815 observations in each monthly bin is given above each maximum value. The dashed line  
 816 indicates the hypoxia criterion of  $62.5 \text{ mmol O}_2 \text{ m}^{-3}$ . Observations are from Rabalais et al.

817 (2007), Lehrter et al. (2009, 2012), Nunnally et al. (2012), Murrell et al. (2013b), and the  
818 MCH program.



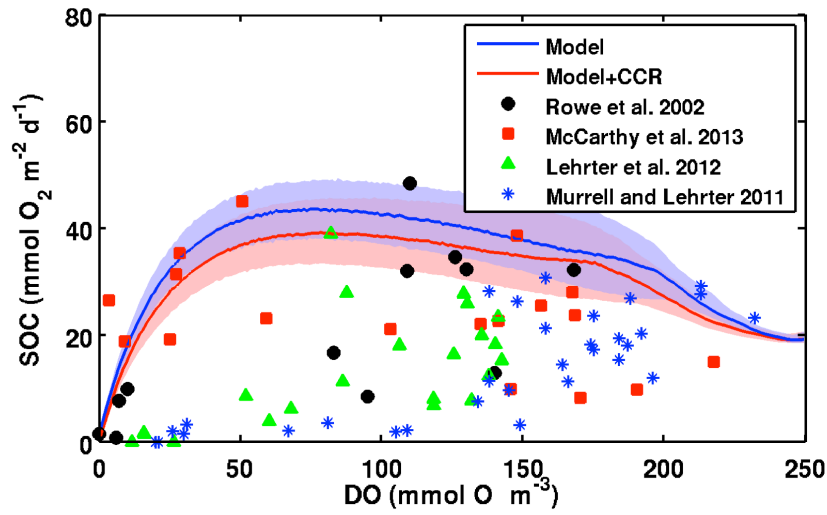
819  
820 **Fig. 5.** Vertical profiles of model bias (model minus observations,  $\text{mmol O}_2 \text{ m}^{-3}$ ) in  
821 dissolved oxygen (DO) calculated from 2004 to 2007 for June to August in the 4 sub-  
822 regions. The vertical axis is the scaled depth, where 0 corresponds to the surface and -1 to  
823 the bottom. The light grey areas represent the standard deviation in the observations.  
824 Observations are from Rabalais et al. (2007), Lehrter et al. (2009, 2012), Murrell et al.  
825 (2013b), and the MCH program.



826

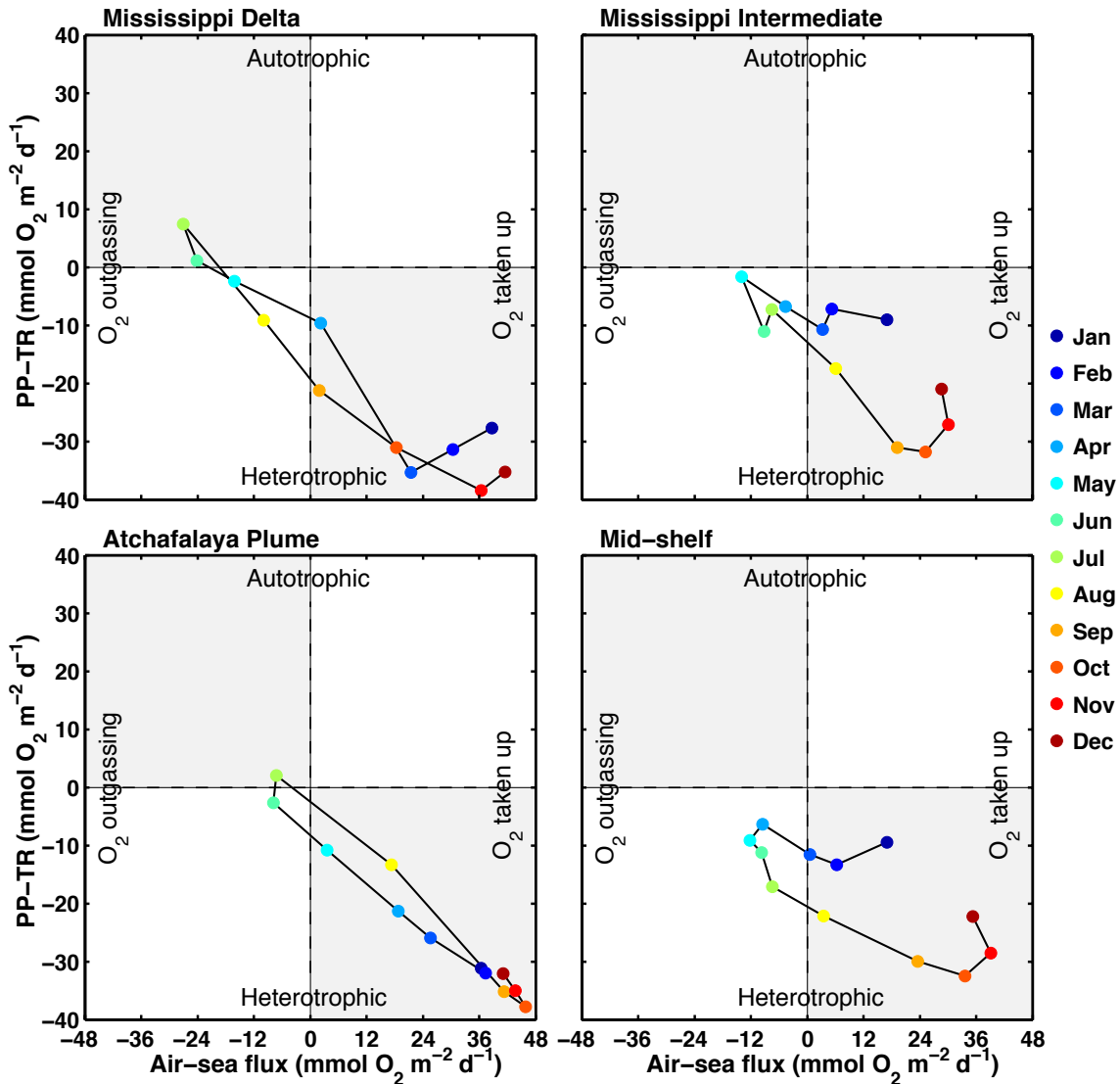
827 **Fig. 6.** Vertically integrated rates of observed and simulated primary production (upper  
 828 panel) and water column respiration (lower panel) in the 4 sub-regions. The error bars  
 829 indicate the standard deviation. The number of observations in each sub-region is given  
 830 above the error bars.

831



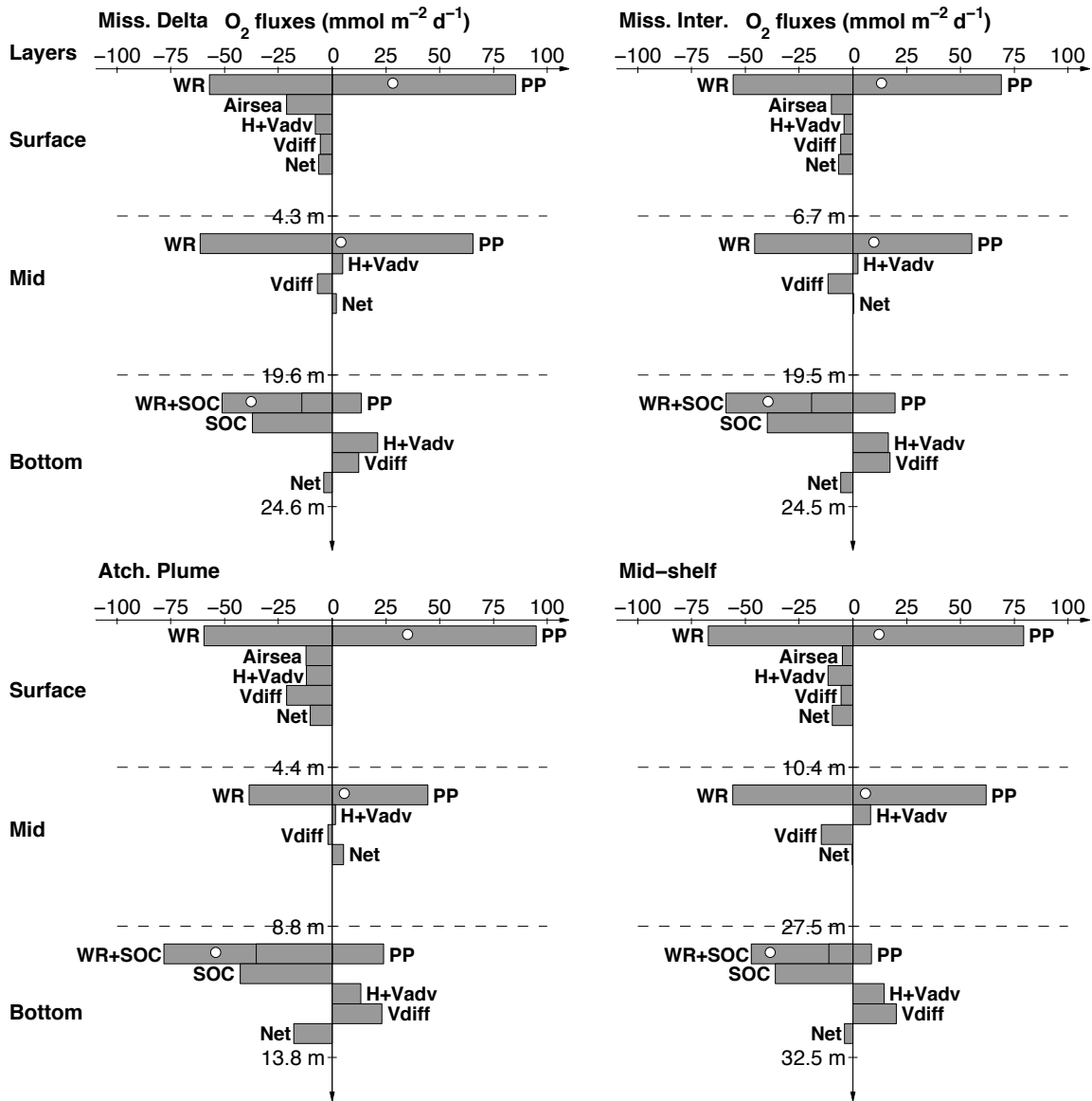
832

833 **Fig. 7.** Model simulated sediment oxygen consumption (SOC) versus bottom dissolved  
 834 oxygen (DO) for the period 2004 to 2007, including the median (solid line) and the range  
 835 between 25th and 75th percentiles (shaded area). Also shown for comparison are  
 836 observations from Rowe et al. (2002), McCarthy (2013), Lehrter et al. (2012) and Murrell  
 837 and Lehrter (2011).



838

839 **Fig. 8.** Simulated net community production (PP-TR) versus air-sea flux of oxygen for  
 840 the 4 sub-regions. The colored dots represent monthly means averaged over 2004 to  
 841 2007. Positive air-sea flux indicates oxygen is taken by water whereas negative air-sea  
 842 flux indicates oxygen outgasses. Positive (PP-TR) suggests autotrophic whereas negative  
 843 (PP-TR) suggests heterotrophic. Standard deviations of the air-sea flux in different  
 844 months and sub-regions range widely from 13 to 58  $\text{mmol O}_2 \text{ m}^{-2} \text{ d}^{-1}$  and standard  
 845 deviation of (PP-TR) range from 12 to 63  $\text{mmol O}_2 \text{ m}^{-2} \text{ d}^{-1}$ , both of which are higher in  
 846 Mississippi Delta and Atchafalaya Plume and lower in the other two regions.

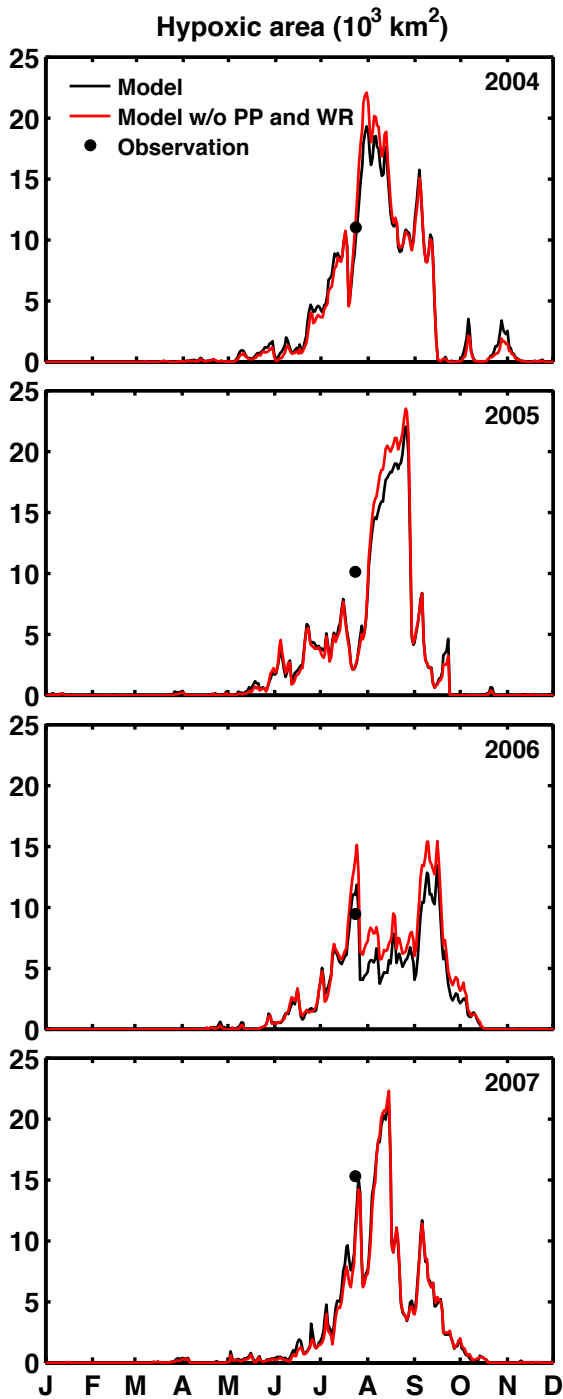


847

848 **Fig. 9.** Simulated 4-year (2004-2007) mean oxygen balance in summer for the 4 sub-  
 849 regions. Oxygen source and sink terms are given for the surface layer above the  
 850 pycnocline, for the mid layer and for the 5-m thick bottom layer. The average depth of  
 851 the pycnocline, depth at 5 m above bottom and the average water column depth are  
 852 indicated for each sub-region. The open circles indicate the balance of primary  
 853 production (PP) and respiration+nitrification (WR) in each layer. For the bottom layer,  
 854 the bars for respiration+nitrification (WR) and sediment oxygen consumption (SOC) are

855 shown stacked and SOC is repeated separately. The net rate of oxygen change in each  
856 layer (i.e. the sum of all oxygen source and sink terms) is given and denoted as Net.

857



858

859 **Fig. 10.** Time series of simulated hypoxic extent for the full model (black line) and the  
860 model without biological processes in the water column (red line). Also shown is the  
861 observed hypoxic extent in late July (black dots). The observed hypoxic extent was  
862 estimated by linearly interpolating the observed oxygen concentrations onto the model  
863 grid and then calculating the area with oxygen concentrations below the hypoxic  
864 threshold (Fennel et al., 2013).